

CONFIDENTIAL

Copy 5
RM L52D15

NACA RM L52D15

SEP 29 1952

UNCLASSIFIED



RESEARCH MEMORANDUM

A PRELIMINARY INVESTIGATION OF THE STATIC AND
DYNAMIC LONGITUDINAL STABILITY OF A
GRUNBERG HYDROFOIL SYSTEM

By Norman S. Land, Derrill B. Chambliss,
and William W. Petynia

Langley Aeronautical Laboratory
Langley Field, Va.

FOR REFERENCE

NOT TO BE TAKEN FROM THIS ROOM

CLASSIFIED DOCUMENT

This material contains information affecting the National Defense of the United States within the meaning of the espionage laws, Title 18, U.S.C., Secs. 793 and 794, the transmission or revelation of which in any manner to unauthorized person is prohibited by law.

NATIONAL ADVISORY COMMITTEE FOR AERONAUTICS

WASHINGTON
September 16, 1952

UNCLASSIFIED

CLASSIFICATION CANCELLED

Authority *24000000-2731* Date *10/12/54*

By *24000000* *11/2/54* See

CONFIDENTIAL

NACA LIBRARY
LANGLEY AERONAUTICAL LABORATORY
Langley Field, Va.



UNCLASSIFIED

NATIONAL ADVISORY COMMITTEE FOR AERONAUTICS

RESEARCH MEMORANDUM

A PRELIMINARY INVESTIGATION OF THE STATIC AND
DYNAMIC LONGITUDINAL STABILITY OF A
GRUNBERG HYDROFOIL SYSTEMBy Norman S. Land, Derrill B. Chambliss,
and William W. Petynia

SUMMARY

A preliminary investigation has been made in order to determine the static and dynamic longitudinal stability characteristics and the force characteristics of a Grunberg hydrofoil system comprising a main lifting hydrofoil and planing-surface stabilizers. The tests showed that a rearward movement of the center of gravity decreased the static and dynamic stability but increased the lift-drag ratio. In smooth water, adequate static stability was observed for all conditions tested. Response to disturbances applied in smooth-water runs showed dynamic stability. In relatively long waves, the model was statically and dynamically stable. As the wave length was decreased, oscillations in trim increased because of bouncing of the stabilizers and the model tended to upset at rearward positions of the center of gravity.

INTRODUCTION

The use of hydrofoils for the sustentation of water-borne craft and for landing gear on water-based aircraft is always of interest because of the relatively high lift-drag ratio obtainable with a submerged hydrofoil in contrast to that attainable with a planing surface. In addition, less pounding in waves would be expected with a hydrofoil than with a planing surface. Relatively little research, however, has been done on the stability of hydrofoil systems or on their behavior in waves.

In order to obtain a better understanding of the influence of design parameters on the stability and resistance characteristics of promising hydrofoil systems, a preliminary investigation was made to determine the static longitudinal stability, the dynamic stability in

UNCLASSIFIED

smooth and rough water, and the force characteristics. An arrangement known as the Grunberg system was chosen for the investigation, as previous tests of such a configuration (refs. 1 and 2) indicated relatively high lift-drag ratios and inherent static stability. The Grunberg system is made up of a hydrofoil which is located just aft of the center of gravity and supports most of the gross weight, and a pair of planing-surface stabilizers located well forward of the center of gravity.

SYMBOLS

a_f	slope of hydrofoil lift curve
a_s	slope of planing-stabilizer lift curve
b	span of hydrofoil, ft
c_a	chord of hydrofoil strut, ft
c_f	chord of hydrofoil, ft
d_a	vertical distance from center of gravity to point of application of resultant drag force on hydrofoil strut, ft
d_f	vertical distance from center of gravity to center of pressure of hydrofoil, ft
d_s	vertical distance from center of gravity to center of pressure of stabilizers, ft
d_t	distance from center of gravity to thrust axis, ft
f	natural frequency, cps
i_f	angle of incidence of hydrofoil (measured between chord and reference line), deg
i_s	angle of incidence of stabilizers (measured between keel and reference line), deg
k	empirical coefficient of additional mass
l	horizontal distance between centers of pressure of hydrofoil and stabilizers, ft
l_{cg}	center-of-gravity location, $\frac{l_s}{l} \times 100$, percent

l_f	horizontal distance between center of gravity and center of pressure of hydrofoil, ft
l_s	horizontal distance between center of gravity and center of pressure of stabilizers, ft
m	empirical coefficient depending on section form, aspect ratio, and other conditions
q	dynamic pressure, $\rho V^2/2$, lb/sq ft
x, y, z	coefficients in differential equation of motion
B	damping factor, ratio of actual damping to critical damping
C_{D_a}	drag coefficient of hydrofoil strut, $D_a/\frac{1}{2}\rho S_a V^2$
C_{D_f}	drag coefficient of hydrofoil, $D_f/\frac{1}{2}\rho S_f V^2$
$C_{D_{0f}}$	drag coefficient of hydrofoil at zero lift
C_{L_f}	lift coefficient of hydrofoil, $L_f/\frac{1}{2}\rho S_f V^2$
C_{L_s}	lift coefficient of stabilizers, $L_s/\frac{1}{2}\rho S_s V^2$
C_M	moment coefficient, $M_{CG}/q S_f c_f$
D_a	drag of hydrofoil strut, lb
D_f	drag of hydrofoil, lb
D_s	drag of stabilizers, lb
I_A	moment of inertia of additional mass of water moving with hydrofoil about stern of stabilizers, slug-ft ²
I_{CG}	moment of inertia of model about center of gravity, slug-ft ²
I_M	moment of inertia of model about stern of stabilizers, slug-ft ²
L_f	lift of hydrofoil, lb
L_s	lift of stabilizers, lb
M_{CG}	sum of moments about center of gravity, lb-ft

M_A	additional mass of water moving with hydrofoil, slugs/cu ft
S_B	immersed area of hydrofoil strut, ft ²
S_F	area of hydrofoil, sq ft
S_S	wetted area of stabilizers, sq ft
T	thrust, lb
V	forward speed, fps
W	gross load, lb
X	amplitude of oscillation, radians
α_F	angle of attack of hydrofoil (measured from zero-lift line), deg
α_S	angle of attack of stabilizers, deg
ρ	mass density of water, (1.972 slugs/cu ft)
θ	angular displacement from equilibrium, radians
$\dot{\theta}$	angular velocity, radians/sec
$\ddot{\theta}$	angular acceleration, radians/sec ²
τ	trim (angle between reference line and horizontal), deg

DESCRIPTION OF MODEL

The model, designated Langley tank model 270, consisted of a skeleton framework sufficient to mount the hydrofoil, stabilizers, and necessary ballast. No hull or fuselage was provided since, in the speed range of interest, the hull would be above the free-water surface. Any effects of a hull or fuselage are beyond the scope of this paper. A general-arrangement drawing of the model is presented in figure 1 and photographs in figures 2 and 3.

The gross weight of the model was chosen as 100 pounds, the length between the quarter-chord point of the hydrofoil and the stern of the stabilizers as 3.75 feet, and the design top speed as 75 feet per second. The area of the hydrofoil (0.178 square foot) was that necessary to

support the total gross load at 75 feet per second, with an arbitrarily selected lift coefficient of 0.1. In order to reduce the effect of the proximity of the free-water surface, the design incidence of the hydrofoil was such that the tips would be submerged approximately 1 chord at the top speed. An aspect ratio of 10 was selected as the highest consistent with structural requirements, resulting in a span of 16 inches and a chord of 1.6 inches. The hydrofoil was constructed with an NACA 64A412 section, 10° dihedral, and an unswept rectangular plan form. The single central supporting strut had a symmetrical circular-arc section, was slightly tapered in plan form, and had a fineness ratio of 8 at the hydrofoil. Both the strut and the hydrofoil were made of stainless steel and were heat-treated. No attempt was made to fillet the intersection of strut and hydrofoil.

Since the model was to be operated with a constant water-borne load throughout the speed range, it was known that the angle of attack of the hydrofoil and stabilizers would vary with the speed. Observations of a previous model (ref. 2) showed that this angle-of-attack variation occurred as a rotation in trim of the model, the center of this rotation being located approximately at the stern of the stabilizers. This fact, together with the length of the model and the desired maximum angle of attack, determined the minimum length of hydrofoil strut. The maximum angle of attack was that necessary to support the load at the minimum speed, which was arbitrarily selected as 25 feet per second.

The stabilizers shown in figure 4 were investigated. One set had a length-beam ratio of 3, a transverse stern, and a constant angle of dead rise of 20° . The keel and chines were parallel for a distance of 2 beams forward of the stern. During the course of the tests, these stabilizers were modified to a length-beam ratio of 4 by reducing the beam to 3.45 inches. These latter stabilizers are shown on the model in figure 2. The third set of stabilizers had a length-beam ratio of 8, a sharply pointed stern, and a warped angle of dead rise. These stabilizers are shown on the model in figure 3. For the dynamic-stability test, the model was self-propelled with thrust provided by an electric motor and propeller mounted on the towing staff. The pitching moment of inertia of the model was varied by redistributing the ballast.

APPARATUS AND PROCEDURE

Unless otherwise stated on figures, the test conditions were: gross load, 100 pounds; angle of incidence of the hydrofoil, 0° ; angle of incidence of stabilizer, 7.6° .

Dynamic-Stability Tests

For the investigation of dynamic stability, the towing gear was that generally used for tests of dynamic models of flying boats. This apparatus (fig. 1) allows the model to have freedom in trim, rise, and fore-and-aft position relative to the towing carriage.

Dynamic stability in smooth water was investigated at constant speeds with and without applied disturbances. One disturbance consisted of an increase and sudden removal of an increment of load that was sufficient to change the trim approximately 3° from equilibrium. For the second type of disturbance, the stabilizers were lifted clear of the water and then suddenly released.

The dynamic stability in rough water was investigated at constant speed in oncoming waves approximately 2.5 inches high with wave lengths ranging from 10 to 28 feet. Waves of this height could not be generated in regular trains with wave lengths shorter than 10 feet.

For the stability tests, the oscillations of the model in trim and rise were recorded against time by use of slide-wire pickups in conjunction with a recording oscillograph.

Force Tests

For the measurements of resistance, the model was towed free-to-trim under the main carriage of tank no. 1. The apparatus and methods used are described in reference 3. Variables considered were: longitudinal location of the center of gravity, incidence of hydrofoil and stabilizers, and gross load. A maximum-speed range of 25 to 70 feet per second was investigated. A windscreen in front of the model reduced aerodynamic tares to a negligible value.

ANALYSIS OF LONGITUDINAL STABILITY

Static Stability

The forces acting upon a Grunberg system are shown in figure 5. The moment of these forces about the center of gravity is given by

$$M_{CG} = -L_f l_f + L_s l_s - D_f d_f - D_s d_s - D_a d_a - T d_t \quad (1)$$

where bow-up moments are considered positive in sign. The assumption is made that there are no air or water forces acting on portions of the craft above the free-water surface other than those of the propeller. Since the dimensions of the hydrofoil and stabilizers are small compared with their distances from the center of gravity, changes in moment arm due to center-of-pressure shift are neglected; therefore, the forces are considered to be acting from the stern of the stabilizers and the quarter-chord point of the hydrofoil. The lateral position of the stabilizers and the depth of the hydrofoil are assumed to be such that the hydrofoil is not in the wake of the stabilizers.

The lift of the hydrofoil L_f may be expressed as

$$L_f = C_{L_f} q S_f = a_f \alpha_f q S_f$$

The effects of cavitation and depth below the surface on the hydrofoil forces are neglected, as the design operating conditions were chosen to minimize such effects.

The lift of the planing-surface stabilizers is

$$L_s = C_{L_s} q S_s$$

The lift curves for a planing surface with dead rise are not straight lines, as may be seen in figure 6, which shows the lift data for a planing surface with 20° angle of dead rise (derived from ref. 4). These curves may be approximated by straight lines, however, with sufficient accuracy over the useful range of trim, so that the equation

$$L_s = a_s \alpha_s q S_s$$

may be used. It should be noted that the wetted area S_s is not a fixed quantity. That is, a given load may be supported at a given speed over a range of angle of attack since the wetted area changes. This is in contrast to a submerged lifting element with a fixed wetted area.

The drag of a hydrofoil may be expressed as

$$D_f = C_{D_f} q S_f$$

The drag coefficient is approximately a function of the square of the angle of attack, so that

$$D_f = (C_{D_{O_f}} + m\alpha_f^2)qS_f$$

The drag of the stabilizers cannot be as conveniently expressed mathematically as the other forces on the system. Figure 7 (taken from ref. 4) shows the lift-drag ratio of a planing surface with a 20° angle of dead rise. For simplicity, the lift-drag ratio of the stabilizers is assumed to be constant over the trim range of interest and to have a value of 5.8. The drag of the stabilizers is then

$$D_s = \frac{L_s}{5.8} = \frac{1}{5.8} a_s \alpha_s q S_s$$

The strut drag is

$$D_a = C_{D_a} q S_a$$

The strut drag coefficient will not vary greatly with attitude as the only effect of attitude is a small change in the effective fineness ratio of the section. Therefore, the strut drag is approximated by

$$D_a = C_{D_a} q c_a (d_f - d_s)$$

The assumption is made that the propulsion force T and its moment around the center of gravity will not vary as the craft is displaced slightly from an attitude of equilibrium.

Substituting these expressions for the forces in the moment equation (1),

$$M_{CG} = -a_f \alpha_f q S_f l_f + a_s \alpha_s q S_s l_s - (C_{D_{O_f}} + m\alpha_f^2) q S_f d_f - \frac{1}{5.8} a_s \alpha_s q S_s d_s -$$

$$C_{D_a} q c_a (d_f - d_s) d_a - T d_t \quad (2)$$

The angles of attack of the hydrofoil and stabilizers may be related to the trim of the craft by their angles of incidence. The term $2.8/57.3$ is necessarily included in the relation between the trim and hydrofoil angle of attack and is the angle between the zero-lift line and chord line of the hydrofoil in radians. Then

$$M_{CG} = -a_f \left(\tau + i_f + \frac{2.8}{57.3} \right) q S_f l_f + a_s (\tau + i_s) q S_s l_s -$$

$$\left[C_{D_{of}} + m \left(\tau + i_f + \frac{2.8}{57.3} \right)^2 \right] q S_f d_f - \frac{1}{5.8} a_s (\tau + i_s) q S_s d_s -$$

$$C_{D_a} q c_a (d_f - d_s) d_a - T d_t$$

If

$$M_{CG} = C_M q S_f c_f$$

the equation can be put in coefficient form:

$$C_M = -a_f \left(\tau + i_f + \frac{2.8}{57.3} \right) \frac{l_f}{c_f} + a_s (\tau + i_s) \frac{S_s l_s}{S_f c_f} -$$

$$\left[C_{D_{of}} + m \left(\tau + i_f + \frac{2.8}{57.3} \right)^2 \right] \frac{d_f}{c_f} - \frac{a_s}{5.8} (\tau + i_s) \frac{S_s d_s}{S_f c_f} -$$

$$C_{D_a} \frac{c_a}{c_f} \frac{d_f - d_s}{S_f} d_a - \frac{T d_t}{q S_f c_f} \quad (3)$$

Differentiating with respect to τ yields

$$\frac{dC_M}{d\tau} = -a_f \frac{l_f}{c_f} + a_s \frac{S_s l_s}{S_f c_f} - 2m \frac{d_f}{c_f} \left(\tau + i_f + \frac{2.8}{57.3} \right) - \frac{a_s}{5.8} \frac{S_s d_s}{S_f c_f} \quad (4)$$

Therefore,

$$\frac{dC_m}{d\tau} = -a_f \frac{l_f}{c_f} + a_s \frac{S_s}{S_f} \frac{l_g}{c_f} - 2m\alpha_f \frac{d_f}{c_f} - \frac{a_s}{5.8} \frac{S_s}{S_f} \frac{d_s}{c_f} \quad (5)$$

If $dC_m/d\tau$ is negative in sign, the system will be statically stable and the magnitude of $dC_m/d\tau$ is a measure of the degree of stability.

From equation (5) it may be seen that one important factor influencing the static stability is the longitudinal location of the center of gravity. A rearward movement of the center of gravity decreases the static stability by increasing the value of the destabilizing term (l_g increases) and decreasing the value of the first stabilizing term (l_f decreases). This conclusion is substantiated by the pitching-moment curves shown in figure 8, which were obtained from the test data. The slope of the pitching-moment curves at the trim condition (zero pitching moment) decreases as the center of gravity is moved aft. The model, however, had adequate static stability in smooth water even with the center of gravity at 95 percent of the length. It is believed that the center-of-gravity location will ordinarily be the most important factor in determining the static stability, but for completeness the other factors influencing the stability are discussed in the following paragraphs.

A high slope for the hydrofoil lift curve a_f relative to that for the stabilizers a_s is desirable for high static stability. Such a difference in slopes will probably be the case unless unusual proportions for the hydrofoil and stabilizers are chosen. For example, the slope of the lift curve for a hydrofoil with an aspect ratio of 10 is of the order of 0.08 per degree, whereas the slope of the lift curve for a planing surface with 20° angle of dead rise varies from 0.01 to 0.025 (wetted length-beam ratios of 0.2 and 4, respectively).

The effect of a change in incidence of the stabilizers on the static stability can be deduced from the second, or unstable, term of equation (5). For a given center-of-gravity location and speed, the load carried by the stabilizers is fixed within a narrow range and, as noted before,

$$L_s = a_s \alpha_s q S_s$$

An increase in angle of attack of the stabilizers α_s , accomplished by an increase in their incidence, must then result in a decrease in the product $a_s S_s$, since L_s and q were said to be fixed. The decrease in $a_s S_s$ decreases the value of the destabilizing term and therefore increases the static stability. The fourth term, a stabilizing one, would also be decreased in the same ratio. The effect of this decrease is insignificant since this fourth term is normally much smaller than the destabilizing term. It is believed, however, that the over-all result of a change of incidence of the stabilizers is not large.

By the same reasoning, a change in beam of the stabilizers for a given angle of attack should have no effect on the stability, since the product $a_s S_s$ will not change in value.

Examination of the third term of equation (5) shows that the static stability is increased by increasing the factor m , the strut length, and the operating angle of attack. Factor m may be increased by decreasing the aspect ratio, but this decreases the lift-drag ratio. An increase in the length of the strut d_f would mean an increase in its drag. It also may not be desirable to alter the angle of attack α_f , as it determines the operating lift-drag ratio.

Dynamic Stability in Smooth Water

Observations of the behavior of the model subsequent to a disturbance revealed two modes of oscillation. After a sudden load disturbance, the model returned quickly to equilibrium with only a slight overshoot and the stabilizers remained in contact with the water throughout the oscillation. Lifting the stabilizers clear of the water and suddenly releasing them resulted in an oscillation characterized by a bouncing motion of the stabilizers on the surface of the water. This type of oscillation required several cycles to damp out completely. A simple theoretical analysis of the first type of oscillation is presented in succeeding paragraphs. An analysis of the second type of oscillation has not been made and would be difficult because of the discontinuous force variation on the stabilizers as they enter and leave the water.

The first type of oscillation is analyzed by examining the equation of motion of the system. A rotary motion centered on the stern of the stabilizers was observed in the investigation of reference 2 and is assumed to be present for purposes of this analysis. For simplicity, the thrust and hydrofoil strut drag are assumed to be constant as the system rotates. With the system disturbed through an angle θ from equilibrium trim, the moments about the stern of the stabilizers are due to the following:

- (1) Moment of inertia of the model,

$$I_M \ddot{\theta}$$

- (2) Additional mass of water moving with hydrofoil,

$$I_A \ddot{\theta}$$

where

$$I_A = M_A \left[l^2 + (d_f - d_s)^2 \right]$$

$$M_A = \frac{k\pi c_f^2 b\rho}{4} \quad \text{the additional mass (See ref. 5.)}$$

- (3) Lift increment resulting from angular displacement,

$$\theta a_f q S_f l$$

- (4) Drag increment resulting from angular displacement,

$$\theta \frac{dC_{Df}}{d\alpha_f} q S_f (d_f - d_s)$$

- (5) Lift increment resulting from the vertical component of angular velocity,

$$\dot{\theta} \frac{l}{V} a_f q S_f l$$

- (6) Drag increment resulting from the vertical component of angular velocity,

$$\dot{\theta} \frac{l}{V} \frac{dC_{Df}}{d\alpha_f} q S_f (d_f - d_s)$$

Since the sum of the moments must be zero

$$I_M \ddot{\theta} + I_A \ddot{\theta} + \frac{l}{V} a_f q S_f l \dot{\theta} + \frac{l}{V} \frac{dC_{Df}}{d\alpha_f} q S_f (d_f - d_s) \dot{\theta} + a_f q S_f l \theta +$$

$$\frac{dC_{Df}}{d\alpha_f} q S_f (d_f - d_s) \theta = 0 \quad (6)$$

When terms are collected,

$$(I_M + I_A) \ddot{\theta} + \left[a_f l + \frac{dC_{Df}}{d\alpha_f} (d_f - d_s) \right] \frac{l}{V} q S_f \dot{\theta} + \left[a_f l + \frac{dC_{Df}}{d\alpha_f} (d_f - d_s) \right] q S_f \theta = 0 \quad (7)$$

This type of differential equation describing the free vibrations of a system with damping is discussed at length in many texts, such as reference 6. By substituting for the preceding unwieldy coefficients, the equation may be written

$$x \ddot{\theta} + y \dot{\theta} + z \theta = 0 \quad (8)$$

It can be shown that if $\frac{y^2}{4x^2} - \frac{z}{x} > 0$, the system returns asymptotically to equilibrium. If $\frac{y^2}{4x^2} - \frac{z}{x} = 0$, the system returns to equilibrium in a finite time but with no oscillation. If $\frac{y^2}{4x^2} - \frac{z}{x} < 0$, the system returns to equilibrium by executing damped oscillations.

As an example, for one test condition the model had the following values:

$$a_f = 0.082 \text{ per degree} = 4.70 \text{ per radian (estimated)}$$

$$\frac{dC_{Df}}{d\alpha_f} = 0.00215 \text{ per degree} = 0.123 \text{ per radian (estimated for equilibrium trim of the test condition)}$$

$$l = 3.75 \text{ feet}$$

$$\frac{\rho}{2} = 0.987 \approx 1.0$$

$$d_f = 1.35 \text{ feet}$$

$$d_s = 1.0 \text{ foot}$$

$$V = 40 \text{ feet per second}$$

$$S_f = 0.178 \text{ square foot}$$

$$I_M = 44 \text{ slug-feet}^2 = I_{cg} + \frac{W}{g}(l_s^2 + d_s^2)$$

$$I_A = \frac{k\pi c_f^2 b p}{4} [l^2 + (d_f - d_s)^2] \quad (\text{It will be assumed that } k = 1.0.)$$

$$= \frac{1.33\pi(0.133)^2}{2} [(3.75)^2 + (0.35)^2]$$

$$= 0.525 \text{ slug-feet}^2$$

The use of these values gives:

$$44.5\ddot{\theta} + 470\dot{\theta} + 5020\theta = 0$$

$$\frac{y^2}{4x^2} - \frac{z}{x} = -85$$

so that the model would be expected to execute damped oscillations. The damping of these oscillations is defined by a damping factor B, which is the ratio of the actual damping to the critical damping. Critical damping is the minimum amount of damping which will result in a non-oscillatory (deadbeat) return to equilibrium. The damping factor is expressed by the relation

$$B = \frac{y}{2} \sqrt{\frac{1}{zx}} \quad (9)$$

Substitution of the values previously given for the model yields

$$B = 0.50$$

A somewhat clearer idea of the motion and the significance of so large a damping factor may be gained by computing the ratio of the amplitude of the first overshoot (the maximum amount the model swings past equilibrium) to the amplitude of the disturbance. This ratio is given by

$$\frac{X_2}{X_1} = e^{-\frac{\pi B}{\sqrt{1-B^2}}} \quad (10)$$

where X_2 signifies the overshoot amplitude and X_1 the disturbance amplitude. Substituting the value of $B = 0.50$ into equation (10) yields

$$\frac{X_2}{X_1} = 0.164$$

The motion is very highly damped since the amplitude reduces to only 16 percent of the disturbance amplitude in half of the first cycle. The frequency of these oscillations is

$$f = \frac{1}{2\pi} \sqrt{\frac{z}{x}(1 - B^2)} \quad (11)$$

If the given test quantities are substituted into equation (11), f is found to be 1.46 cycles per second, a value which corresponds to a period of 0.7 second. When the model was operated under the conditions used in these calculations, the motion induced by a load disturbance was recorded and is shown in figure 9. This figure shows that the motion is oscillatory and highly damped, as predicted, and the frequency is of the order of magnitude of the predicted value. The results indicate that this analysis of the simple mode of oscillation of the Grunberg system is useful in making an estimate of the amount of damping present in a given design.

From the coefficients in the differential equation of motion (eq. (7)) and the expression for the damping factor (eq. (9)), the effect of the physical characteristics of the model on the motion following a disturbance may be deduced. The motion will tend to be more highly damped as the over-all length, the hydrofoil area, and the slope of the lift curve

are increased, and as the moment of inertia is decreased. The slope of the drag curve and the strut lengths will have little effect on the motion.

The other mode of oscillation, due to bouncing of the stabilizers, is illustrated in figure 10. The oscillations resulted from lifting the stabilizers clear of the water and releasing them suddenly. In general, the motion was not so well damped as the simple type of motion previously analyzed. The motion appears to be more highly damped with a forward center-of-gravity location, at low speed, and with a low moment of inertia. The frequency of oscillation is higher than for the simple type of motion, the lowest frequency shown being approximately 3.5 cycles per second, with the highest moment of inertia.

It may be concluded that the model, within the range of test variables, showed a very high degree of dynamic stability in smooth water subsequent to a disturbance in gross load and only slightly less stability subsequent to a disturbance to the stabilizers.

A slight self-induced oscillation, due to bouncing or chattering of the stabilizers in smooth water, was noted at the beginning of the test. This oscillation was encountered when the stabilizers with a length-beam ratio of 3 were set at a large angle of incidence and occurred over a speed range from 27.5 to 32.5 feet per second. The motion was principally a trim change of low amplitude (approximately 1° peak-to-peak) and was not due to the presence of any appreciable waves in the tank. A similar oscillation was noted in the tests of reference 2. In the belief that the instability was associated with very low wetted lengths, the stabilizer incidence was reduced and this chattering was no longer observed. The beam of the stabilizers was then reduced (thereby increasing the wetted lengths) and no further chattering occurred during the rest of the tests.

Dynamic Stability in Waves

A short investigation of the behavior of the model in waves was made to determine the effects of three geometrical parameters - center-of-gravity location, moment of inertia, and stabilizer length-beam ratio - and the effects of two operational parameters - speed and wave length.

The effect of speed on the behavior of the model is illustrated in figure 11. The speeds given on the figure are the speeds of the model relative to shore (the speed of advance of the oncoming wave being approximately 7 feet per second). These data indicate that the amplitude of motion became progressively worse as the speed increased. At

3P

the two higher speeds, the stabilizers were bouncing high enough so that they did not contact every wave.

The effect of wave length on the behavior of the model is illustrated in figure 12. The most violent behavior was observed in the shortest wave and was due to severe bouncing of the stabilizers. As the wave length was increased, the bouncing decreased and in the two longest waves the stabilizers followed the surface of the water.

Figure 13 shows the effect of longitudinal location of the center of gravity. The amplitude of motion became progressively worse as the center of gravity was shifted aft until an upsetting condition was reached. This upsetting condition occurs when the amplitude in trim becomes so large that, at the maximum trim during a cycle, the resultant force passes ahead of the center of gravity. This condition is, of course, statically unstable and the upset results. Consequently, with a rearward center-of-gravity location (desirable for high lift-drag ratio) the tendency of the system to upset places a limit on the amplitude of trim motion that can be tolerated.

The effect of moment of inertia on the behavior of the model is shown in figure 14. In the shorter waves, as the moment of inertia was increased, the behavior of the model became so violent that the run had to be stopped. (See fig. 14(a).) In the longer waves, an increase in the moment of inertia seemed to have little effect on the behavior of the model. (See fig. 14(b).) The stabilizers remained on the water at all times when running in the long waves, but bounced, when running in the shorter waves, and in some cases contacted only every other wave. This effect was noted with either moment of inertia.

The effect of changing to stabilizers with a high length-beam ratio, a high angle of dead rise, and a pointed stern is shown in figure 15. Prior to the tests, it was believed that these stabilizers would improve the performance in waves because the impact forces would be less. The test data did not confirm this belief. It was observed during the tests that these stabilizers were completely buried in the waves and larger changes in trim resulted than were observed with the other stabilizers.

FORCE TESTS

The results of the force measurements are shown in figures 16 to 19.

The Reynolds numbers (based on hydrofoil chord) for the force tests varied from 250,000 at 25 feet per second to 700,000 at 70 feet per second. Inasmuch as these Reynolds numbers are low and the extent of

~~CONFIDENTIAL~~

turbulence in the flow over the hydrofoil was not determined, the drag and the lift-drag ratio do not necessarily represent those of a large-scale configuration. These data, however, do show the effects of changes in configuration and the relative importance of these changes.

Light cavitation occurred at the intersection of strut and hydrofoil at speeds of 65 and 70 feet per second. Very light cavitation was noted on the rear portion of the upper surface of the hydrofoil at 70 feet per second.

The effect of stabilizer incidence is shown in figure 16 where lift-drag ratio, total drag, and trim are plotted against speed for four values of the stabilizer incidence. The trim was practically unchanged by a variation in stabilizer incidence of 7° . Little change in trim would be expected since the angle of attack of the hydrofoil, which supported the greater part of the load, was the principal factor determining the trim. As the stabilizer incidence was changed, appreciable differences due primarily to changes in the drag of the stabilizers were found in both the drag and the lift-drag ratio.

A change in the angle of incidence of the hydrofoil (fig. 17) resulted in a trim change which was approximately equal to the change in incidence but in an opposite direction. Thus, the hydrofoil, at a given speed and with a given location of the center of gravity, ran at nearly the same angle of attack (or lift) with either angle of incidence. Therefore, the differences in drag and lift-drag ratio are again primarily due to changes in stabilizer drag.

The increase in gross load from 100 to 125 pounds (fig. 18) resulted in an increase in trim of the model and an increase in lift-drag ratio at high speeds.

The effect of a change in the fore-and-aft location of the center of gravity is shown in figure 19. Shifting the center of gravity rearward increased the lift-drag ratio throughout the speed range. This increase in lift-drag ratio was due to the fact that the hydrofoil, which is more efficient than the stabilizer, carried a larger portion of the total load.

CONCLUSIONS

A preliminary investigation to determine the static and dynamic longitudinal stability characteristics and the force characteristics of a Grunberg hydrofoil system comprising a main lifting hydrofoil and planing-surface stabilizers indicated the following conclusions:

1. The model had good static longitudinal stability at all the conditions investigated.

2. The fore-and-aft location of the center of gravity has an important effect on the static stability and the lift-drag ratio. Moving the center of gravity rearward reduces the static stability but increases the lift-drag ratio.

3. The dynamic stability of the model in smooth water was good. Disturbances caused by a sudden load change resulted in a highly damped oscillation, the characteristics of which were adequately described by simple theory. As the center of gravity moved rearward, the damping decreased. Disturbances to the model caused by lifting the stabilizers and releasing them resulted in bouncing of the stabilizers which damped out in several cycles.

4. The dynamic stability of the model in waves was adversely affected by a rearward movement of the center of gravity, shortening the length of the wave, increasing the speed, and increasing the moment of inertia. A limitation to operation in waves was encountered at rearward positions of the center of gravity, where upsetting resulted when the trim reached such a high value that the resultant force passed ahead of the center of gravity.

5. The maximum total lift-drag ratio for a given configuration occurs approximately at the condition where the hydrofoil is operating at its highest lift-drag ratio. This maximum value is highest if the stabilizers are adjusted to operate at their optimum efficiency at the same condition. This latter adjustment becomes of increasing importance as the proportion of the total load carried by the stabilizers is increased (center of gravity moved forward).

Langley Aeronautical Laboratory
National Advisory Committee for Aeronautics
Langley Field, Va.

REFERENCES

1. Grunberg, V.: La sustentation hydrodynamique par ailettes immergées. Essais d'un système sustentateur autostable. L'Aérotechnique, no. 174, 16^e année, supp. to L'Aéronautique, no. 217, June 1937, pp. 61-69.
2. Land, Norman S.: Tank Tests of a Grunberg Type High-Speed Boat With a Lifting Hydrofoil and Planing Surface Stabilizers. NACA Models 103-A and 103-B. NACA MR, Bur. Aero., July 22, 1940.
3. Truscott, Starr: The Enlarged N.A.C.A. Tank, and Some of Its Work. NACA TM 918, 1939.
4. Shoemaker, James M.: Tank Tests of Flat and V-Bottom Planing Surfaces. NACA TN 509, 1934.
5. Gracey, William: The Additional-Mass Effect of Plates As Determined by Experiments. NACA Rep. 707, 1941.
6. Myklestad, N. O.: Vibration Analysis. McGraw-Hill Book Co., Inc., 1944.

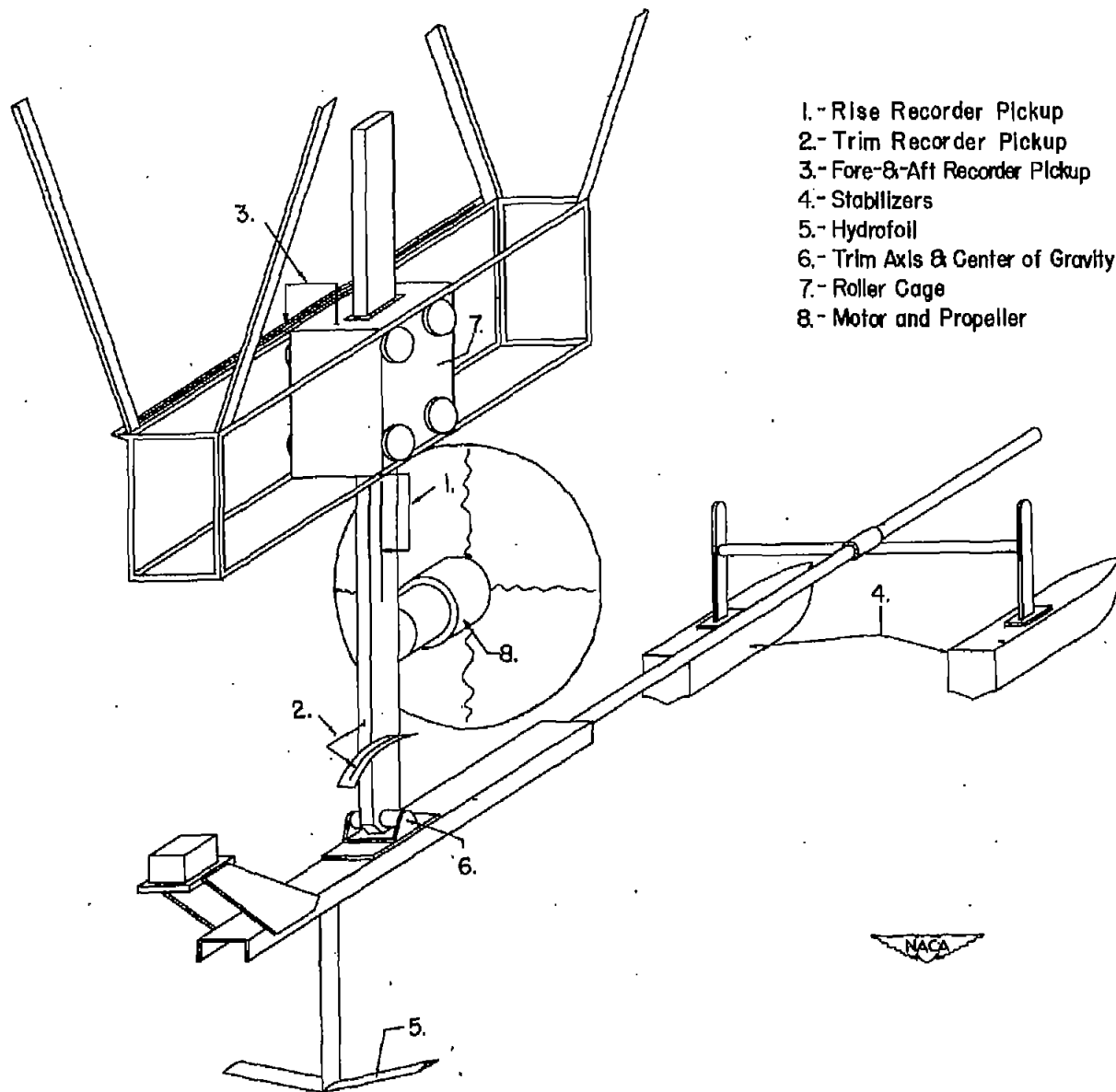


Figure 1.- Langley tank model 270 on dynamic-stability test apparatus.

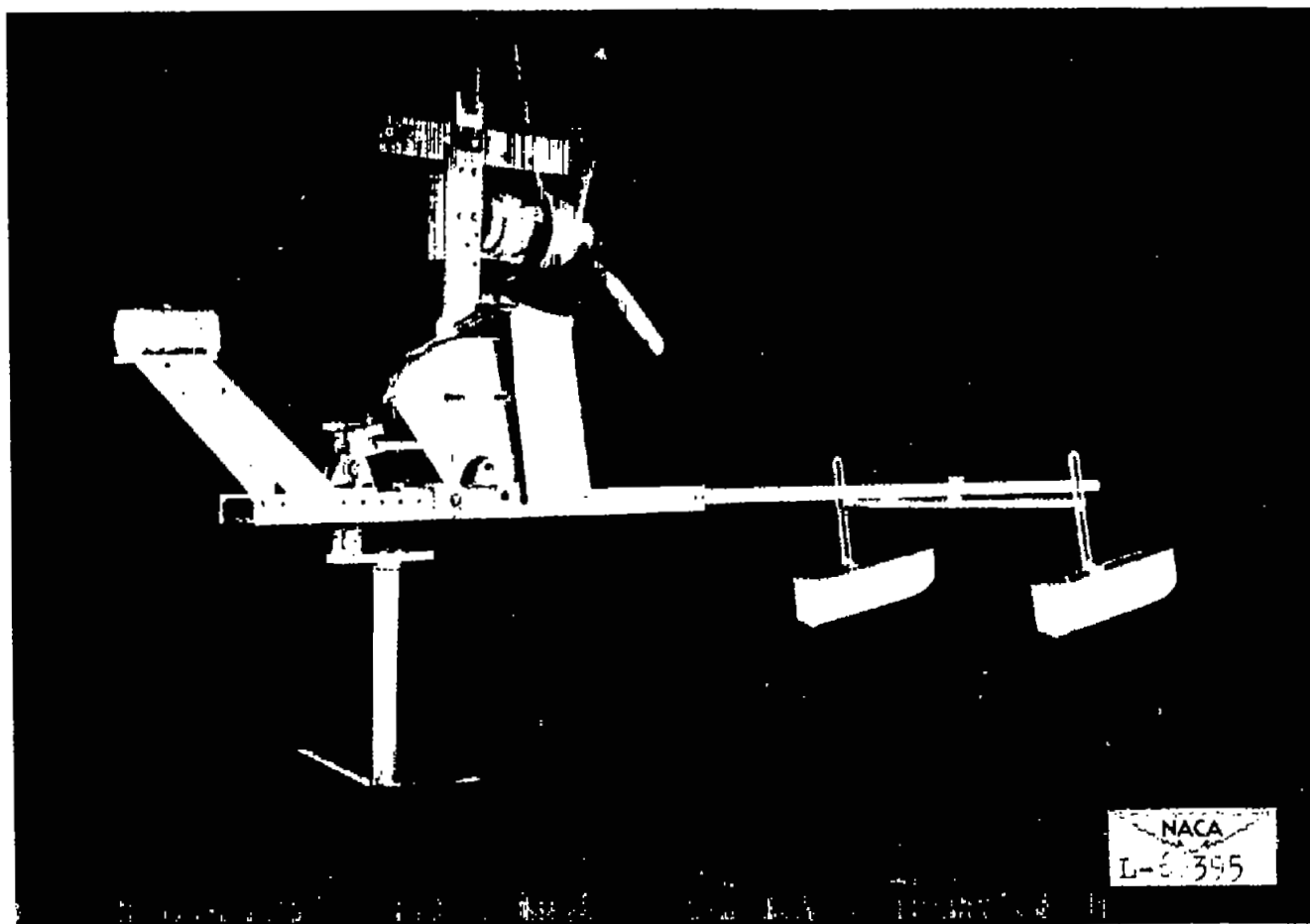


Figure 2.- Langley tank model 270 with stabilizers of low length-beam ratio.

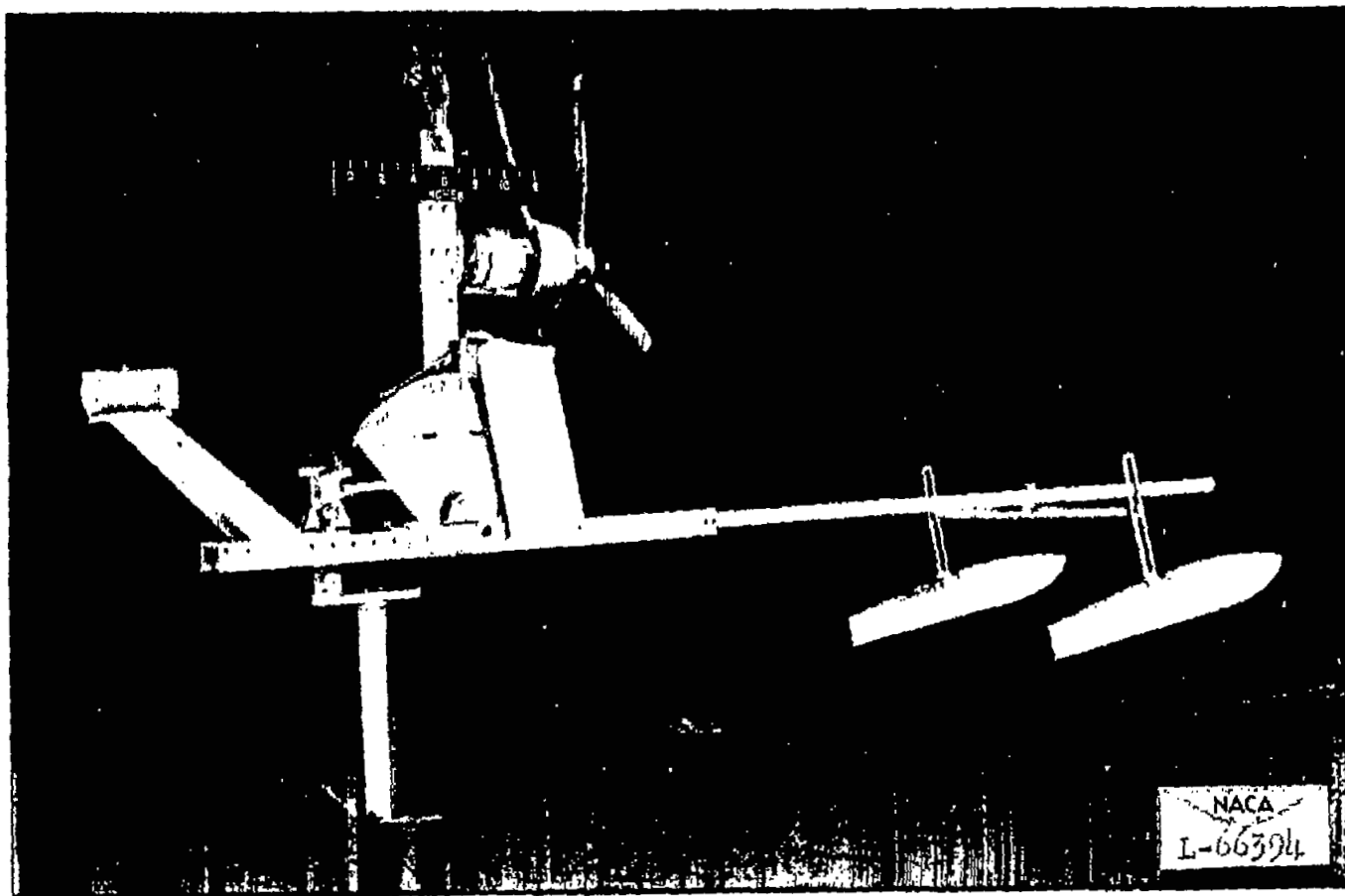
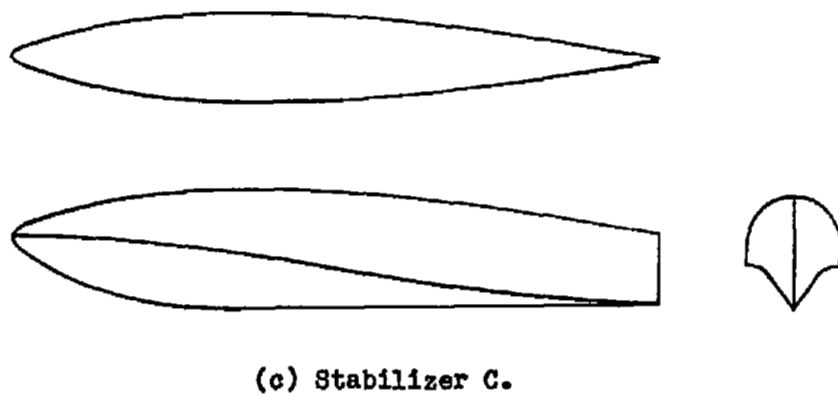
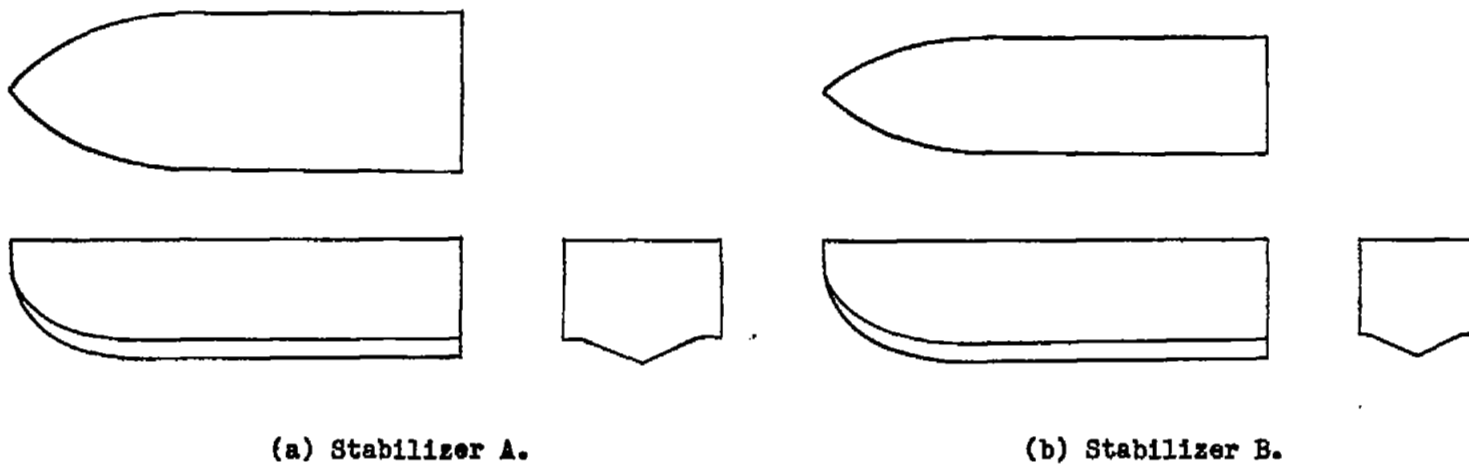


Figure 3.- Langley tank model 270 with stabilizers of high length-beam ratio.



Stabilizer	A	B	C
Length-beam ratio	3	4	8
Length, in.	13.8	13.8	20.0
Beam, in.	4.60	3.45	2.50
Stern dead rise, deg	20°	20°	20°

Figure 4.- Stabilizers of Langley tank model 270.

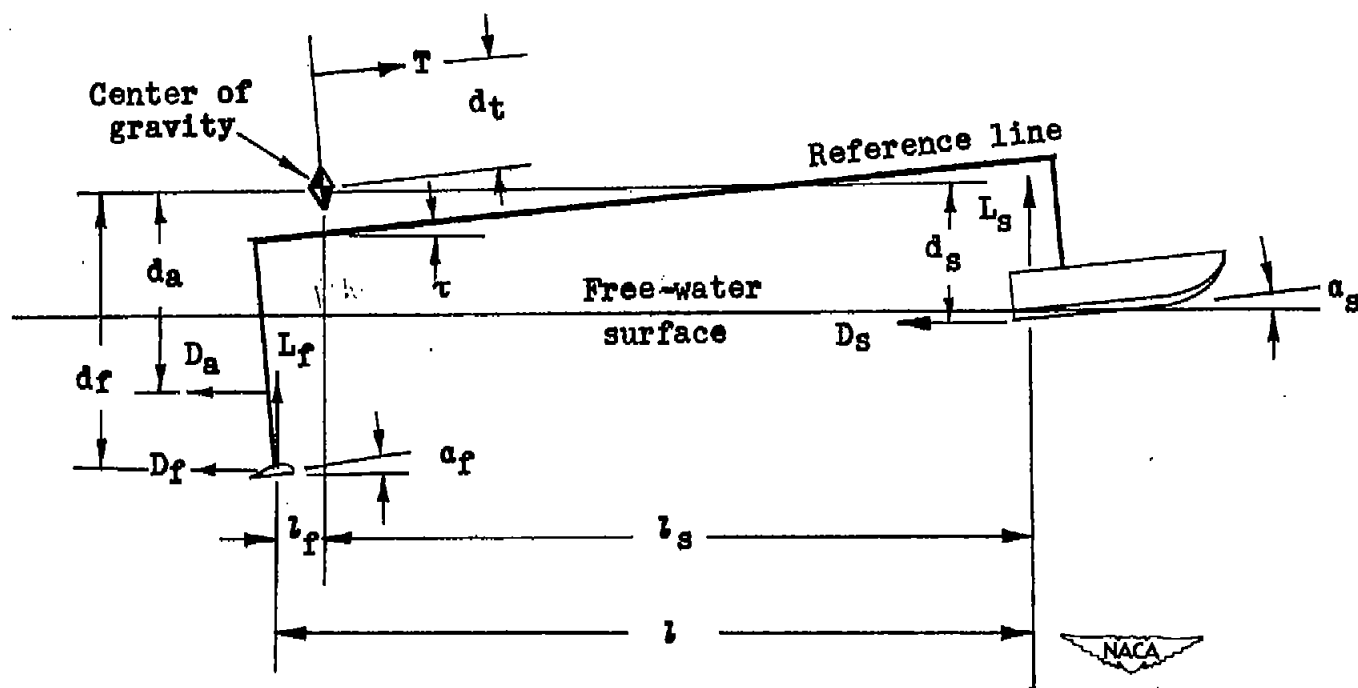


Figure 5.- Forces on Grunberg hydrofoil system.

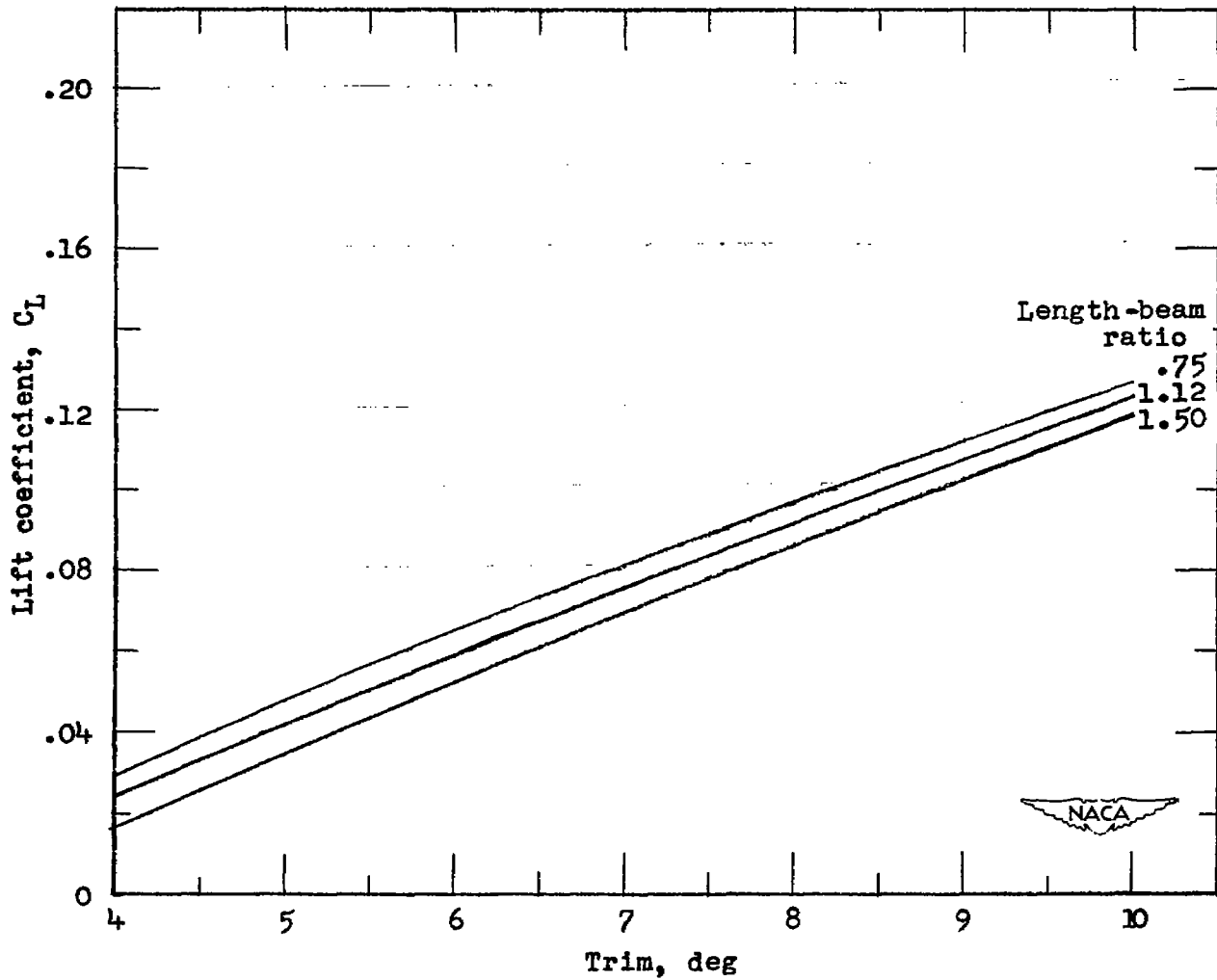


Figure 6.- Characteristic lift for planing surface with 20° angle of dead rise.

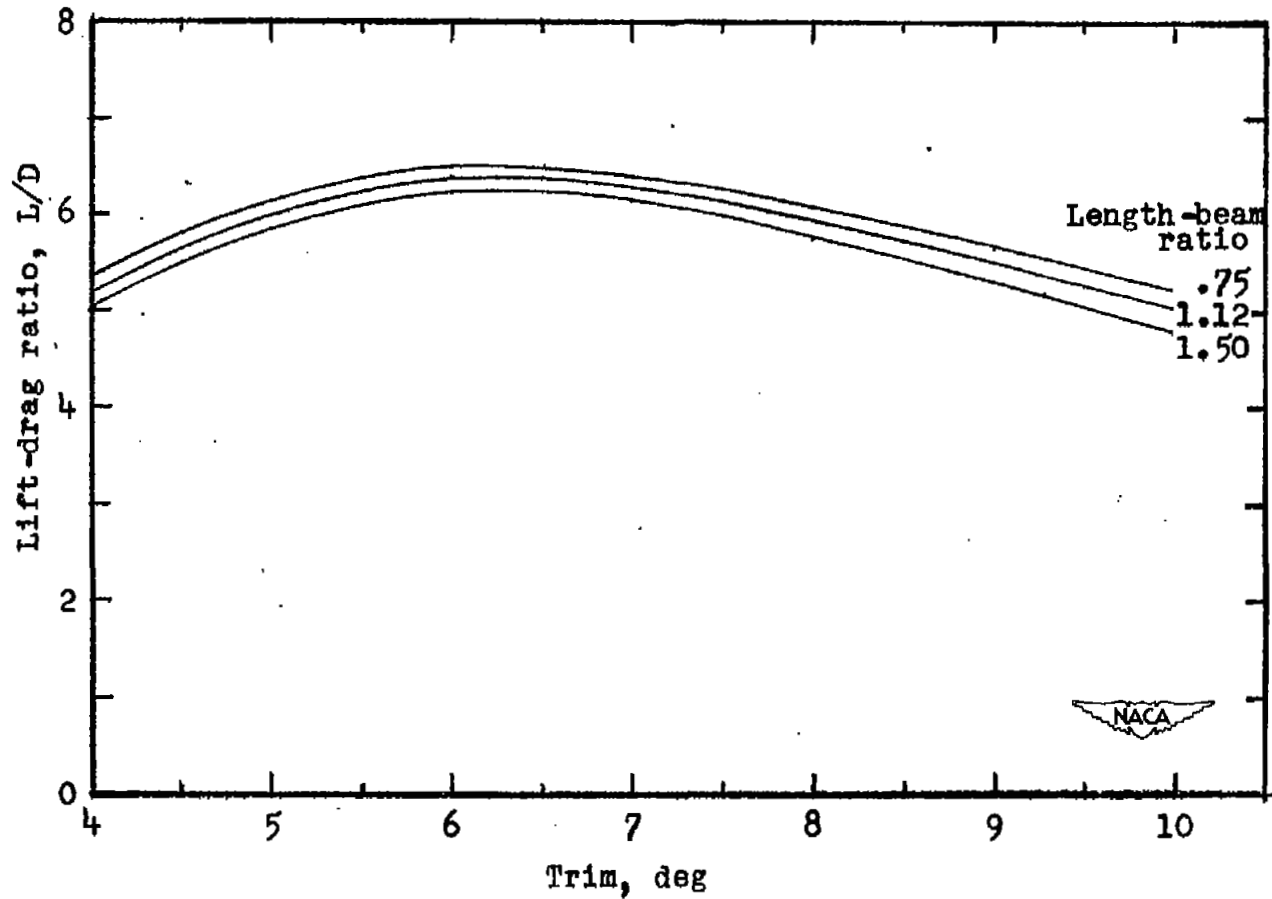


Figure 7.- Characteristic lift-drag ratio for planing surfaces with 20° angle of dead rise (from ref. 4).

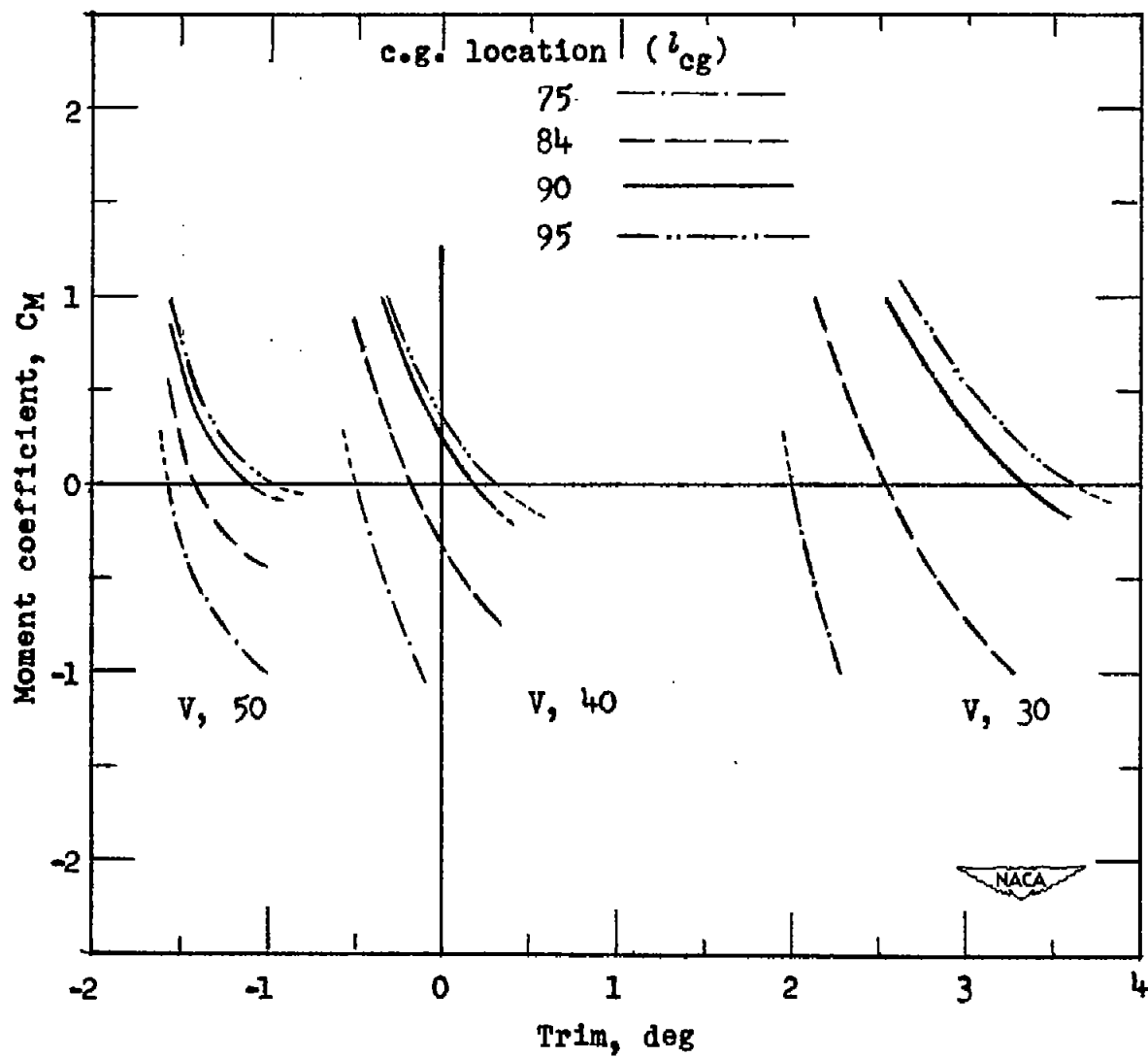


Figure 8.- Hydrodynamic moment coefficient. Stabilizer B.

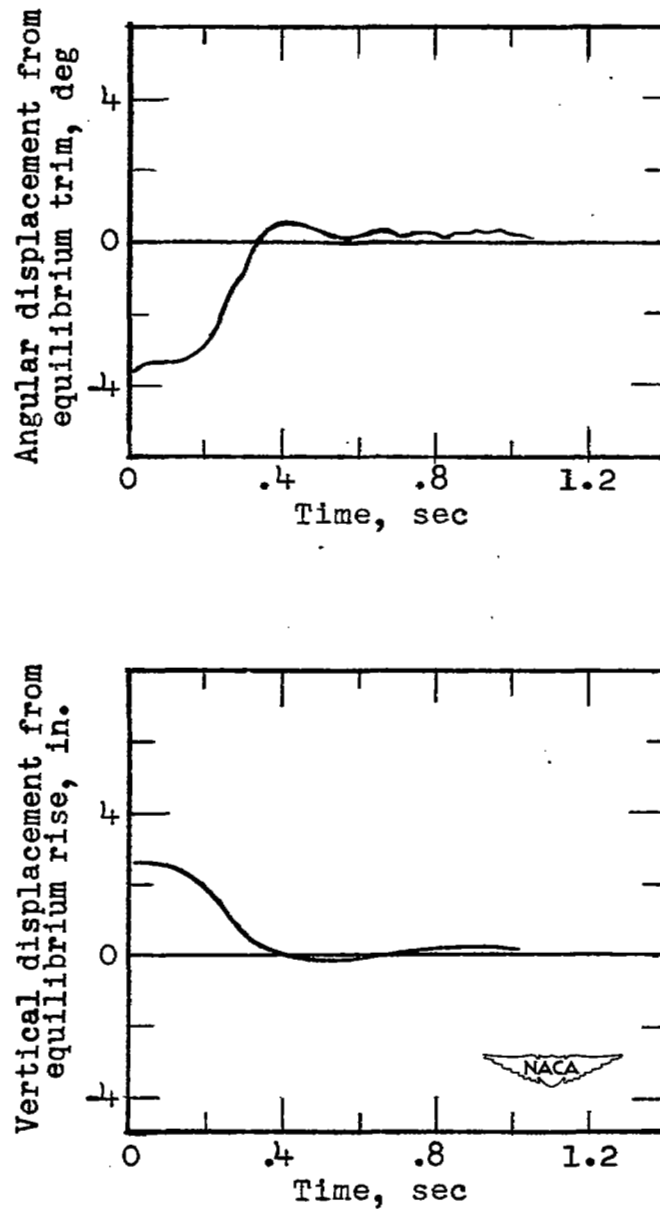


Figure 9.- Load disturbances in smooth water. Stabilizer B; $V = 40$;
 $l_{cg} = 84$.

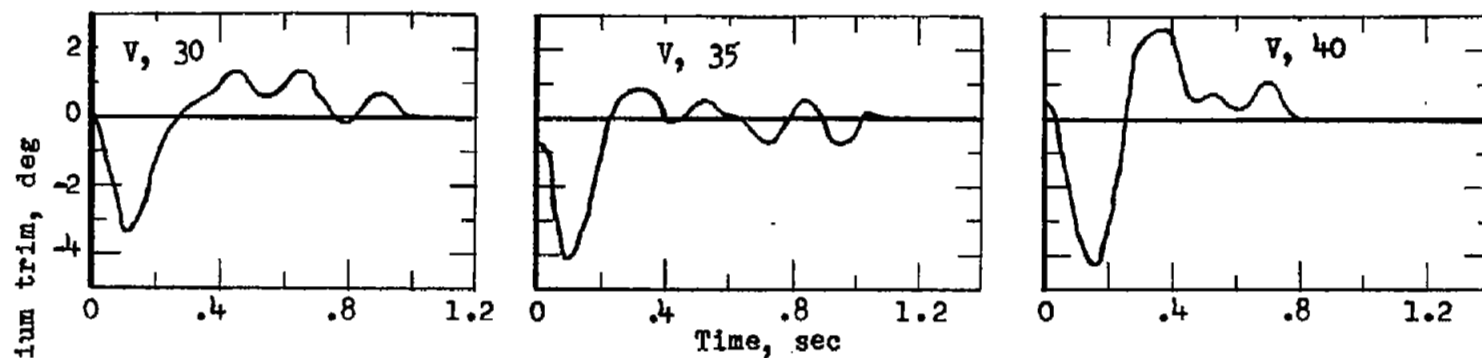
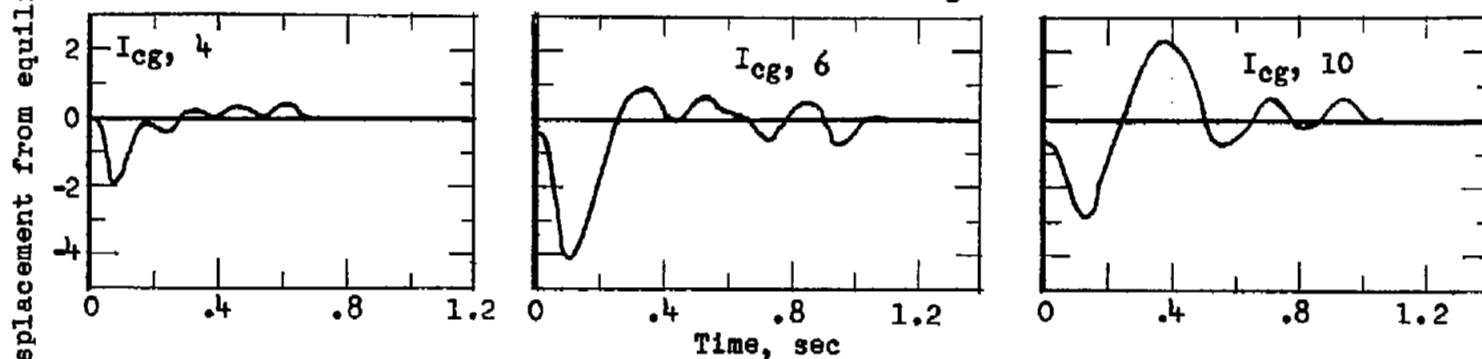
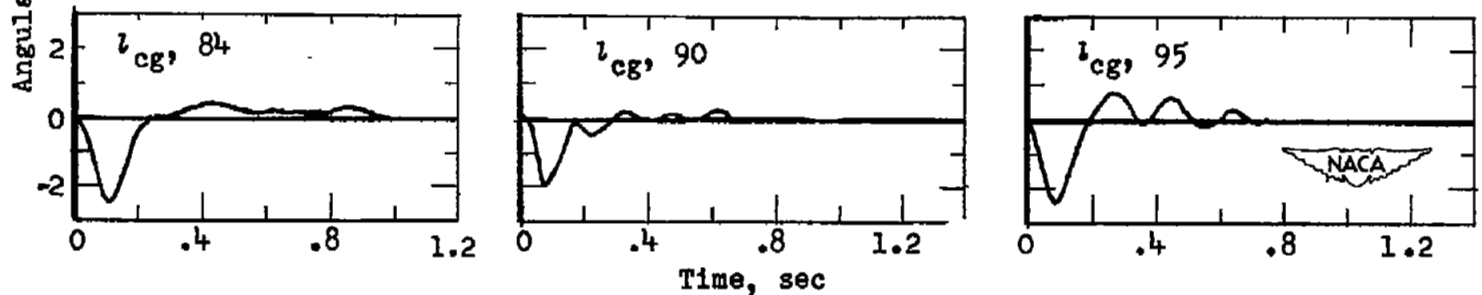
(a) Effect of speed. $I_{cg}, 6$; $l_{cg}, 90$.(b) Effect of moment of inertia. $V = 35$; $l_{cg} = 90$.(c) Effect of center-of-gravity location. $V, 35$; $I_{cg}, 4$.

Figure 10.- Stabilizer disturbances in smooth water. Stabilizer B.

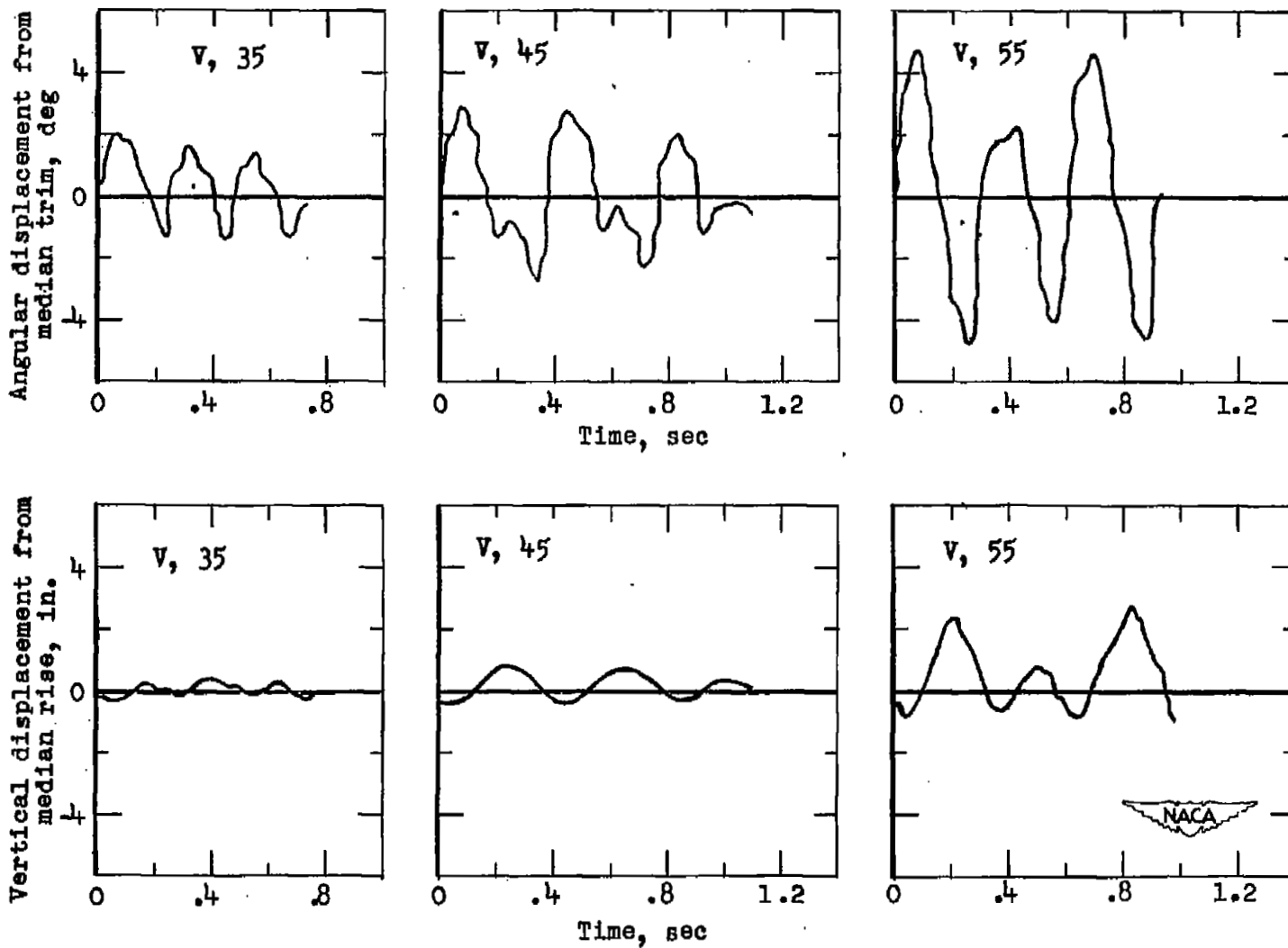


Figure 11.- Effect of speed. Stabilizer B; wave height, 2 inches; wave length, 10 feet; $l_{cg} = 90$; $I_{cg} = 4$.

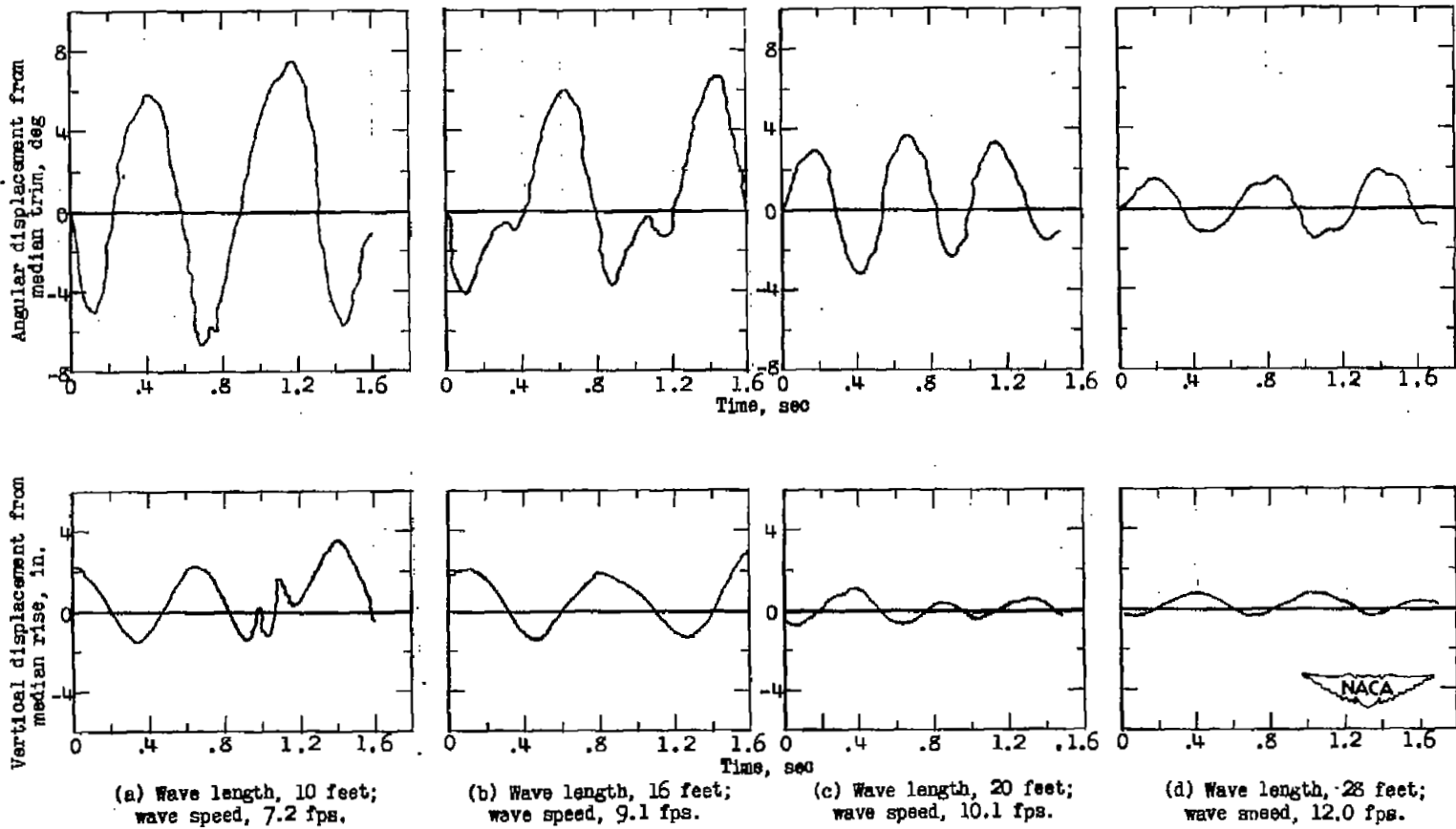


Figure 12.- Effect of wave size. Stabilizer B; $V = 30$; wave height, 2 inches;
 $l_{cg} = 90$; $I_{cg} = 6$.

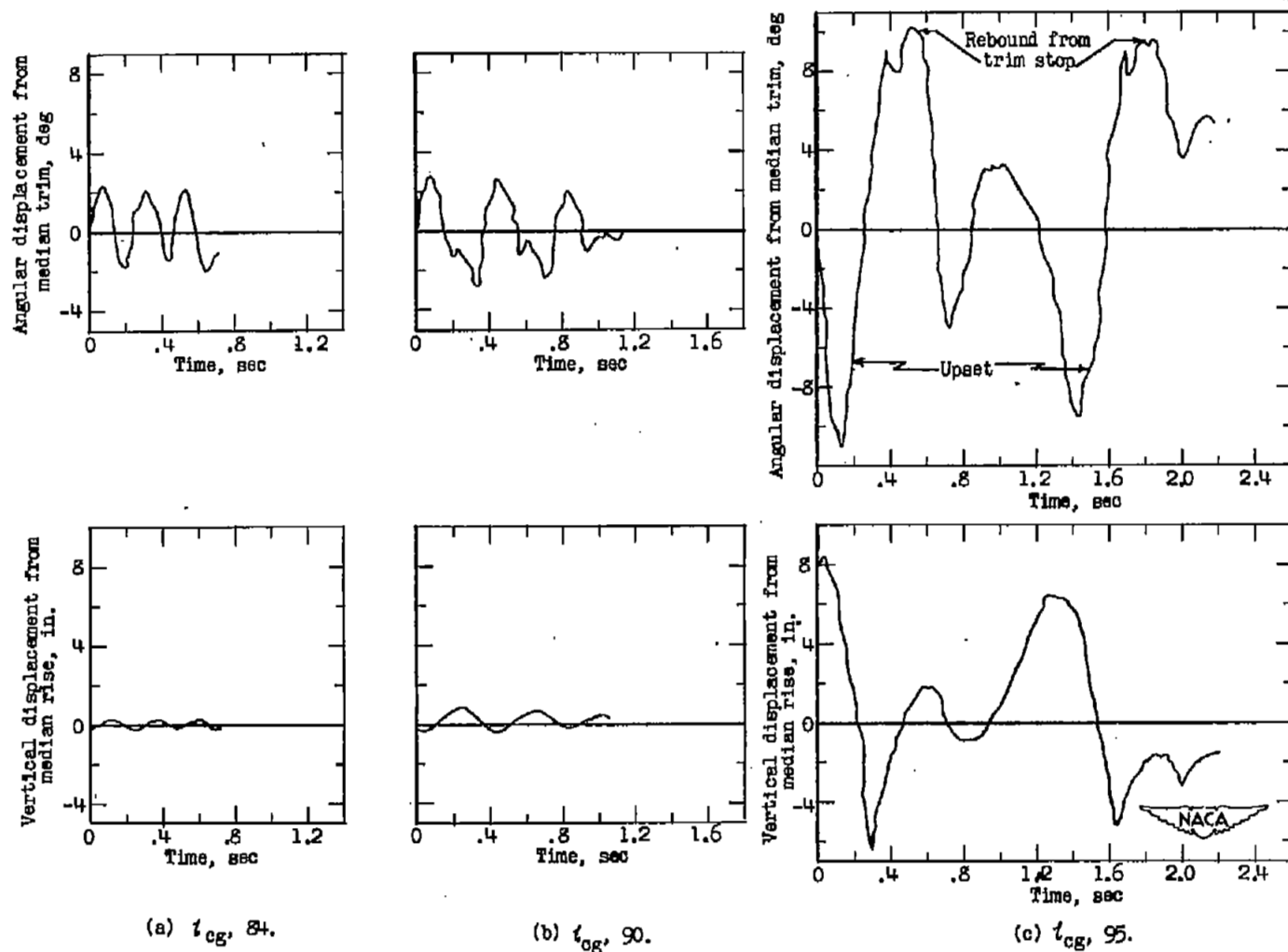
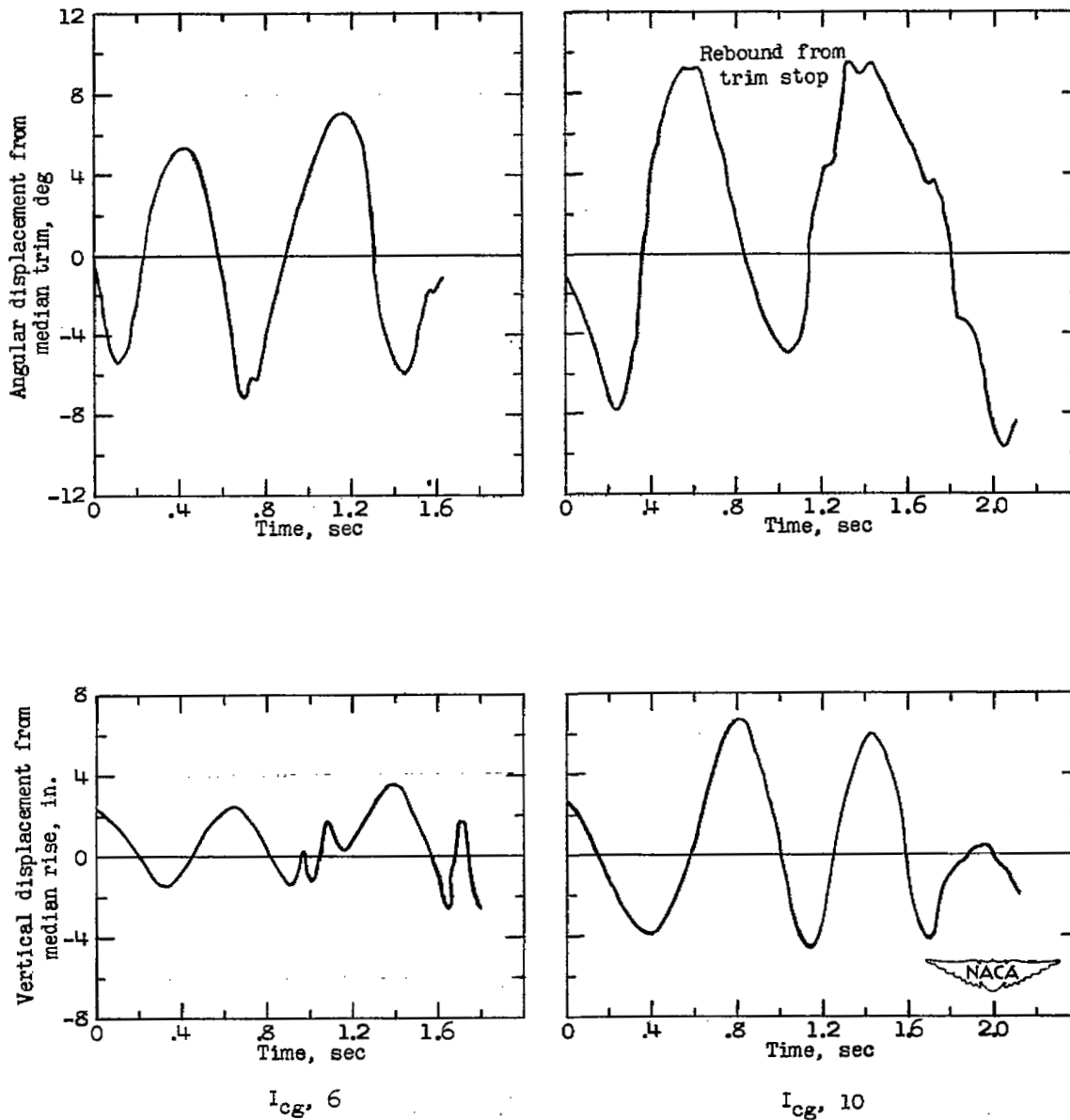
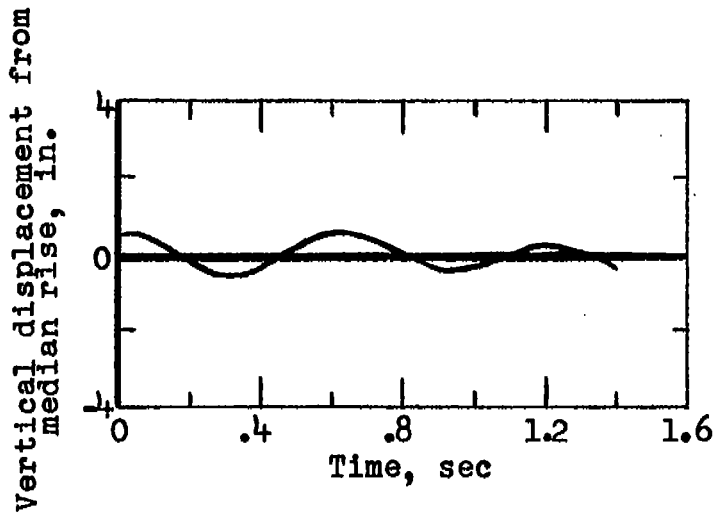
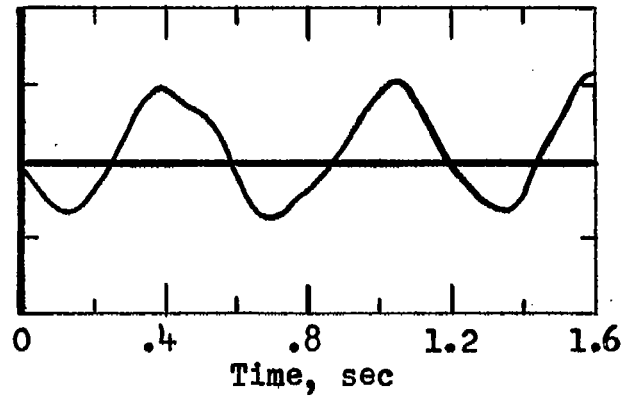
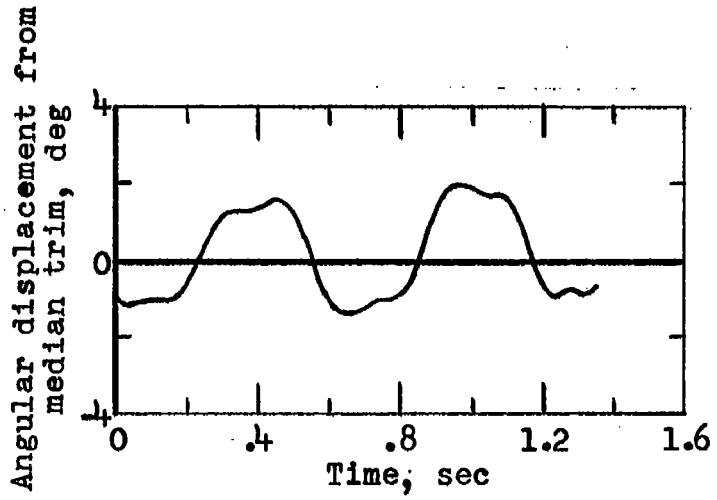


Figure 13.- Effect of center-of-gravity location. Stabilizer B; $V = 35$; wave height, 2.5 inches; wave length, 10 feet; $I_{cg} = 4$.

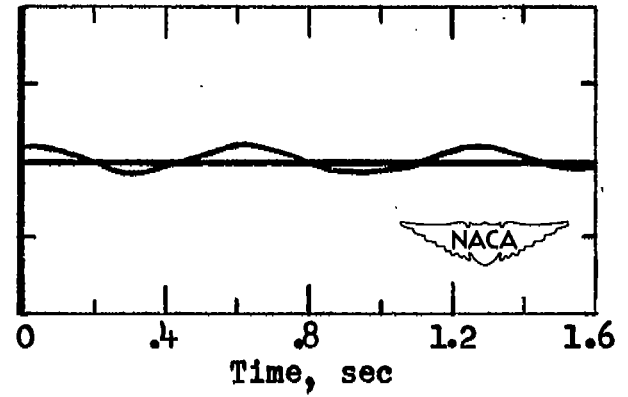


(a) Wave length, 10 feet.

Figure 14.- Effect of moment of inertia. Stabilizer B; $V = 30$; wave height, 2 inches; $l_{cg} = 90$.



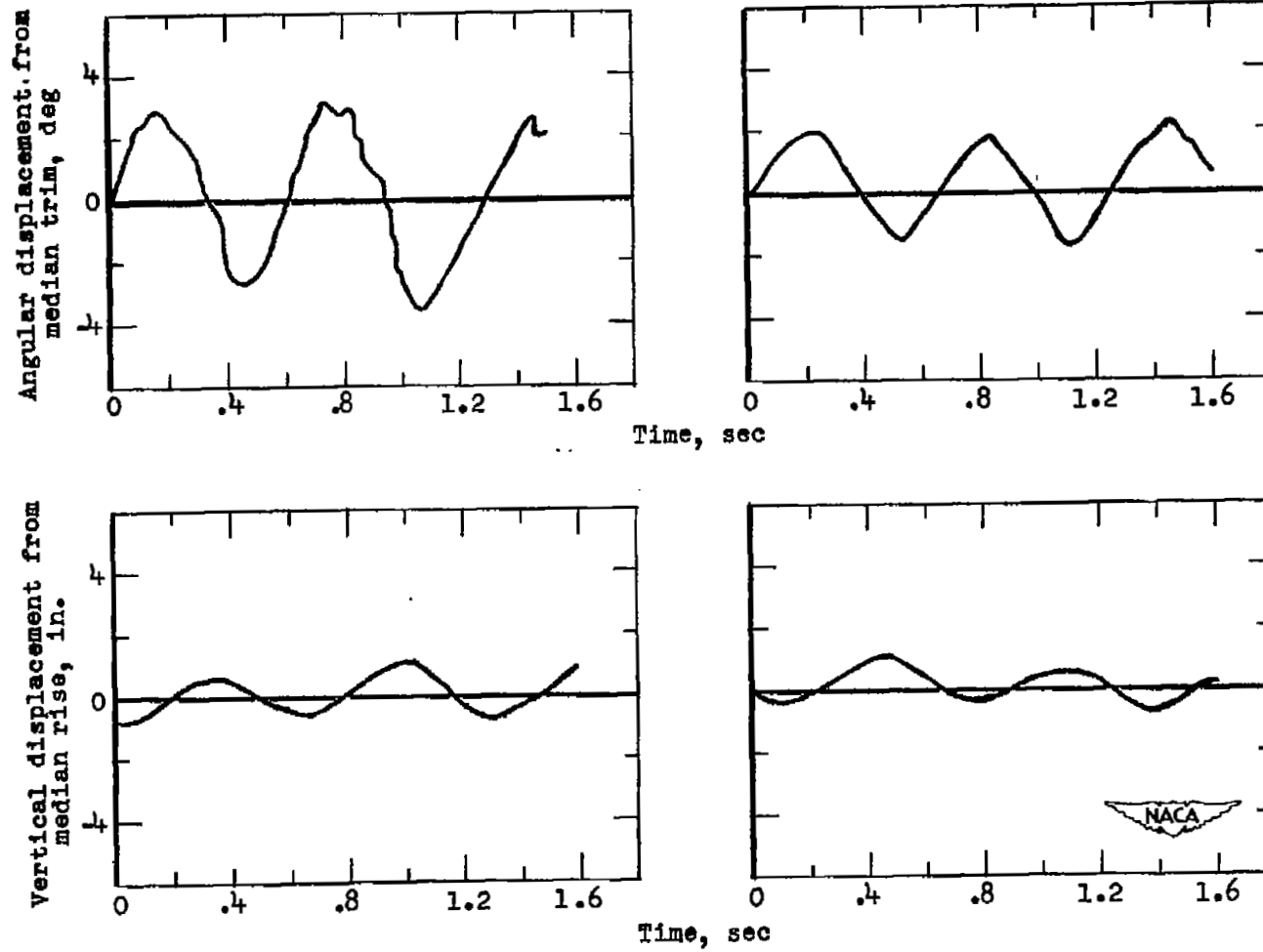
$I_{cg}, 6$



$I_{cg}, 10$

(b) Wave length, 28 feet.

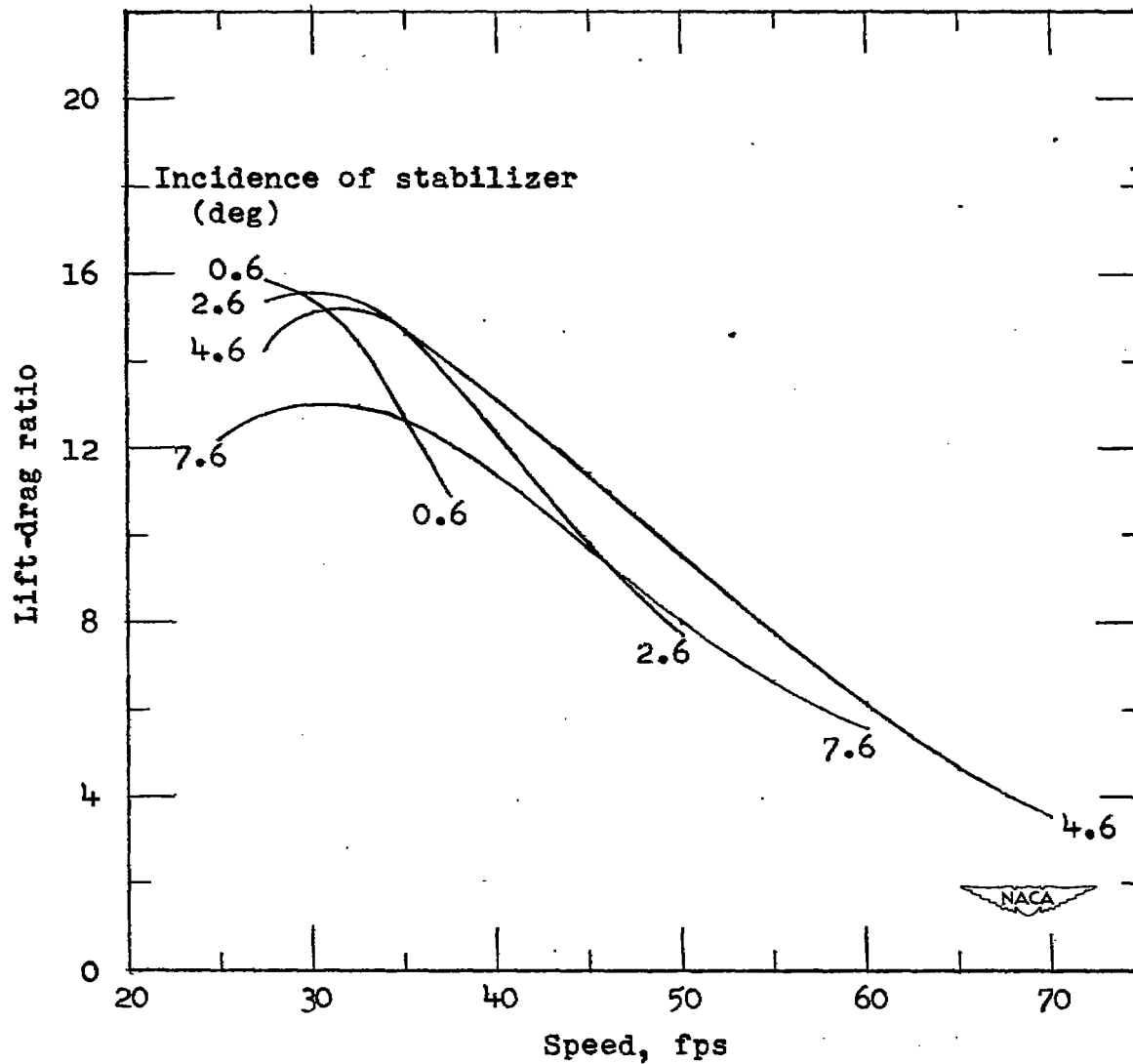
Figure 14.- Concluded.



(a) Stabilizer C.

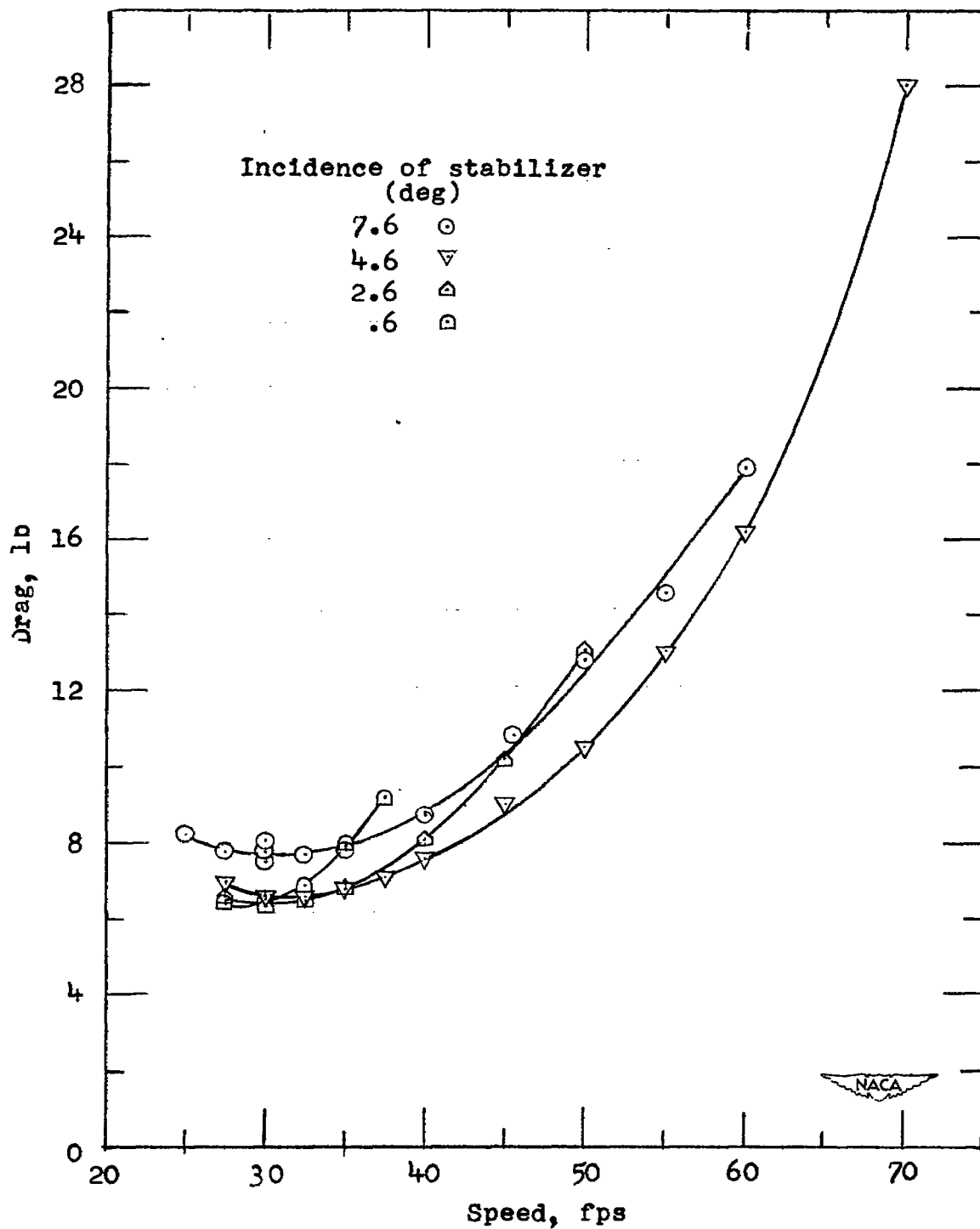
(b) Stabilizer B.

Figure 15.- Effect of a change in stabilizer. $V = 30$; wave height, 2 inches;
 wave length, 28 feet; $l_{cg} = 90$.



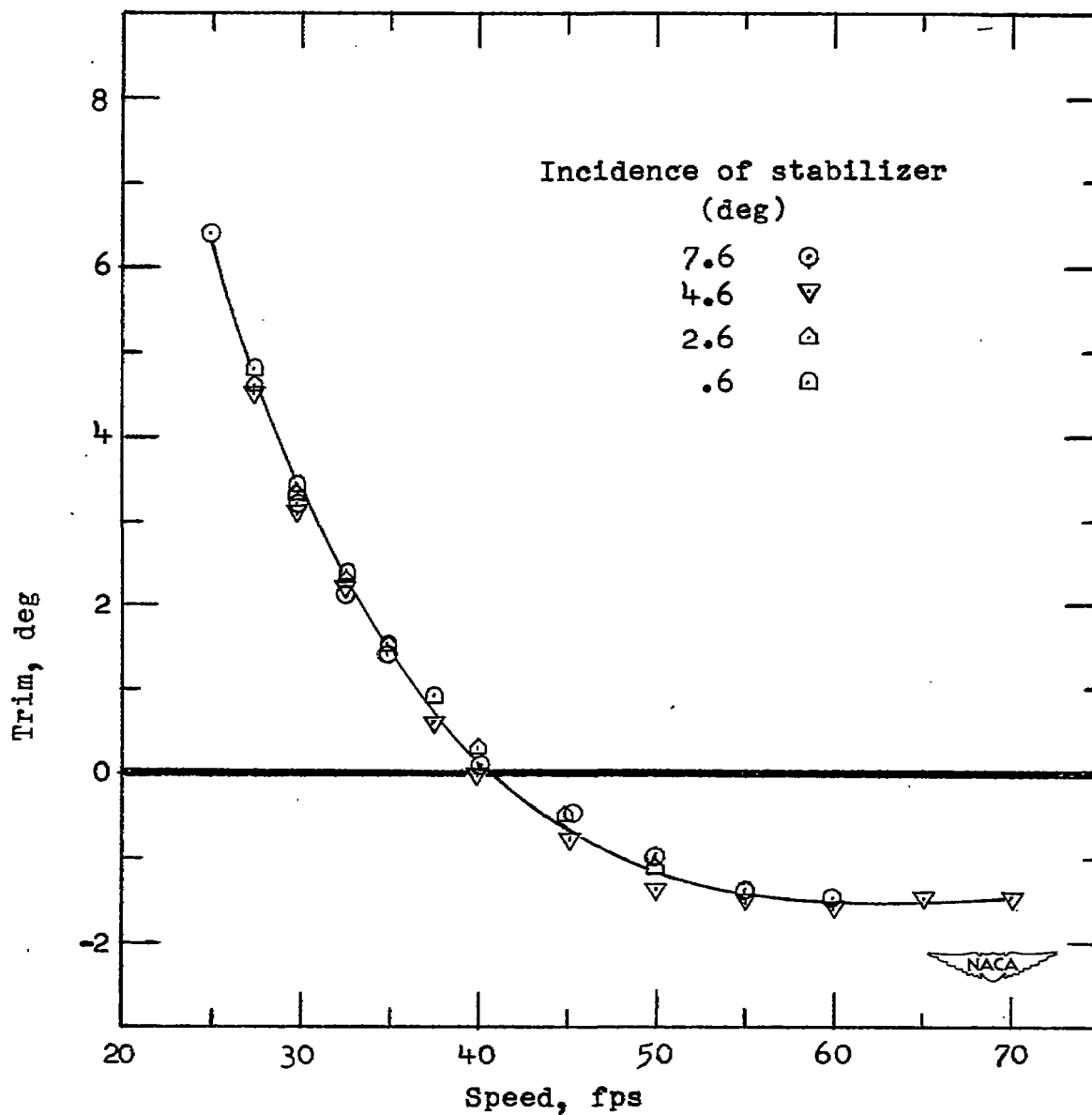
(a) Lift-drag ratio.

Figure 16.- Effect of stabilizer incidence. Stabilizer A; $l_{cg} = 90$.



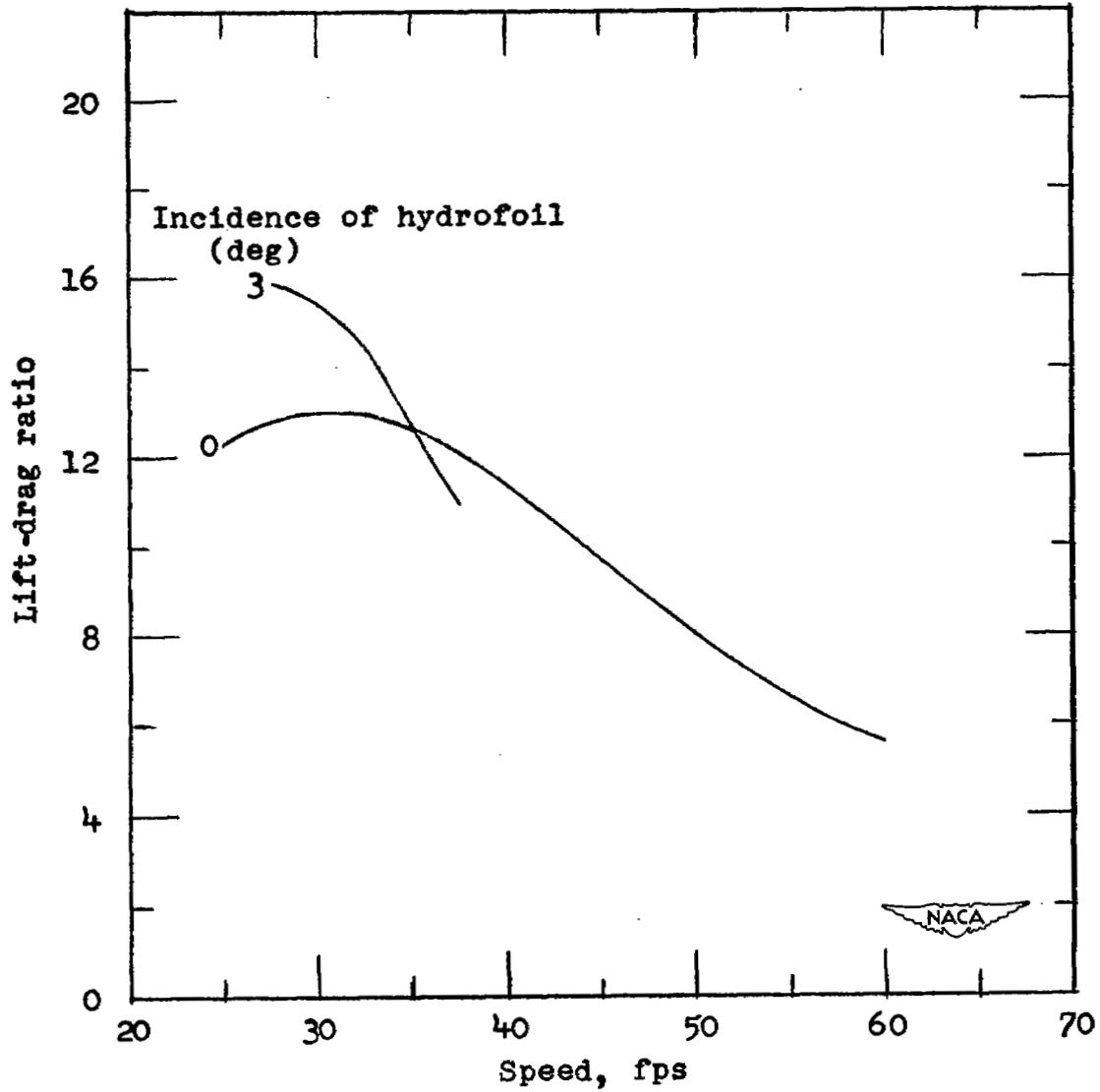
(b) Drag.

Figure 16.- Continued.



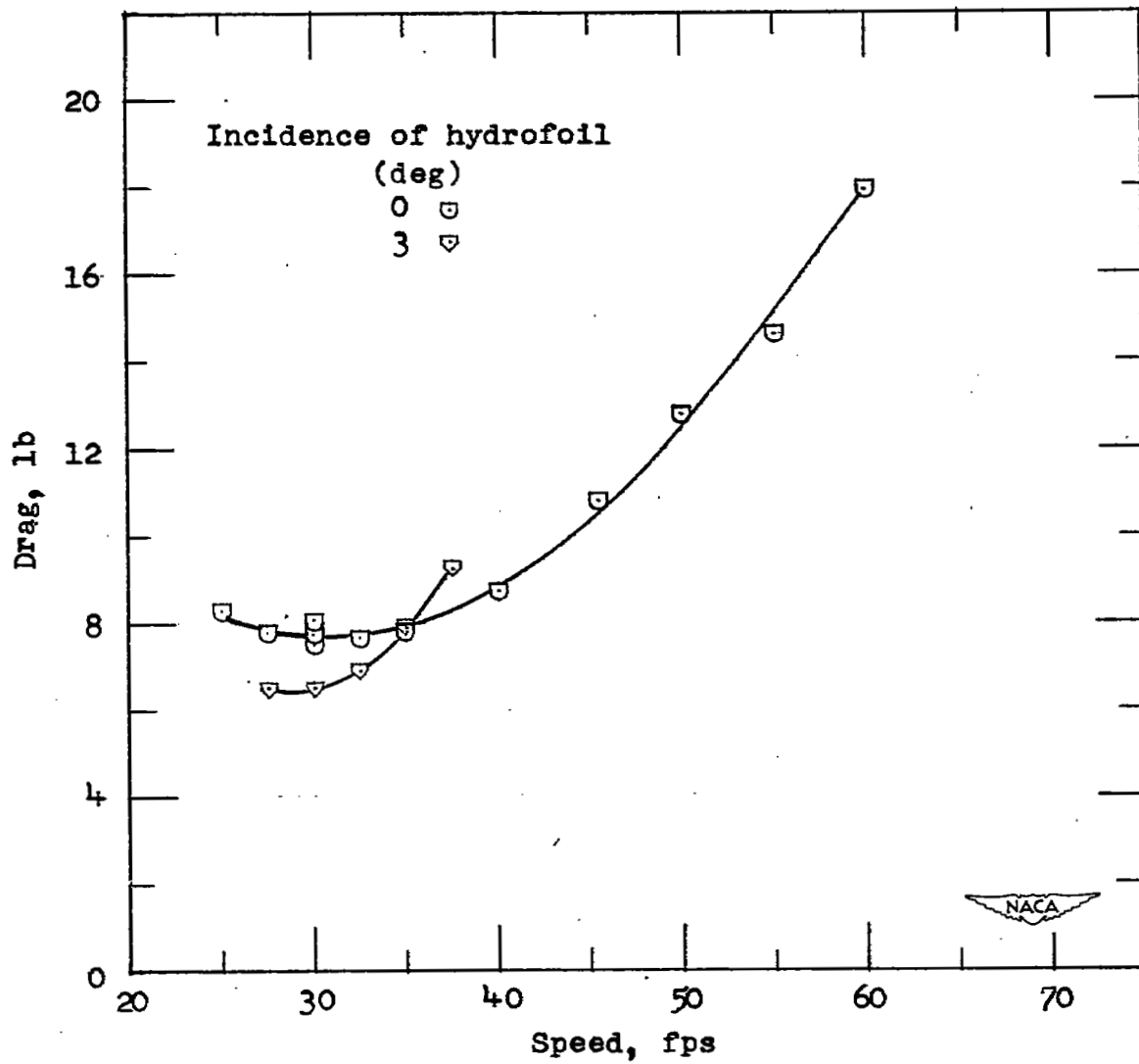
(c) Trim.

Figure 16.- Concluded.



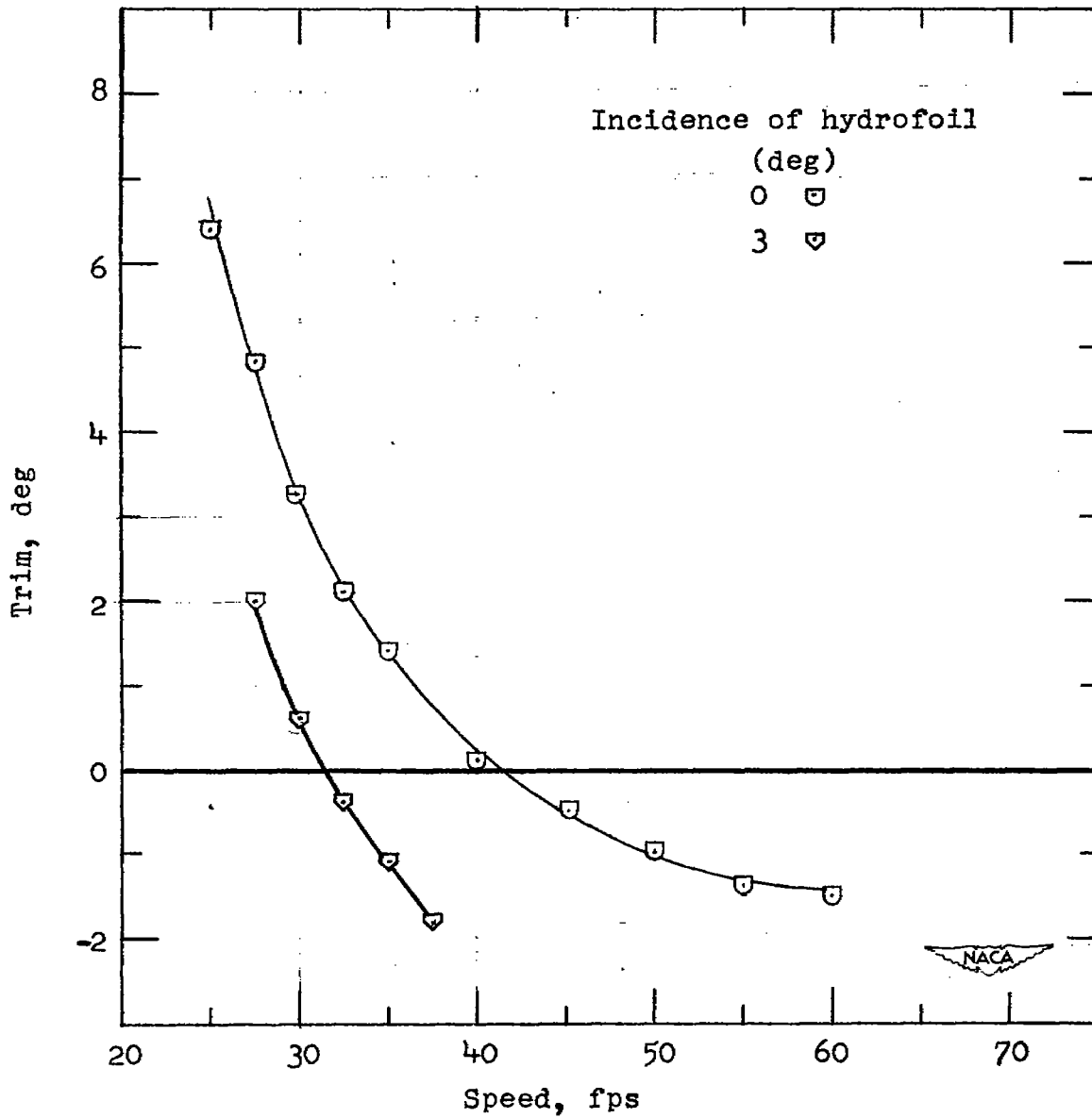
(a) Lift-drag ratio.

Figure 17.- Effect of hydrofoil incidence. Stabilizer A; $l_{cg} = 90$.



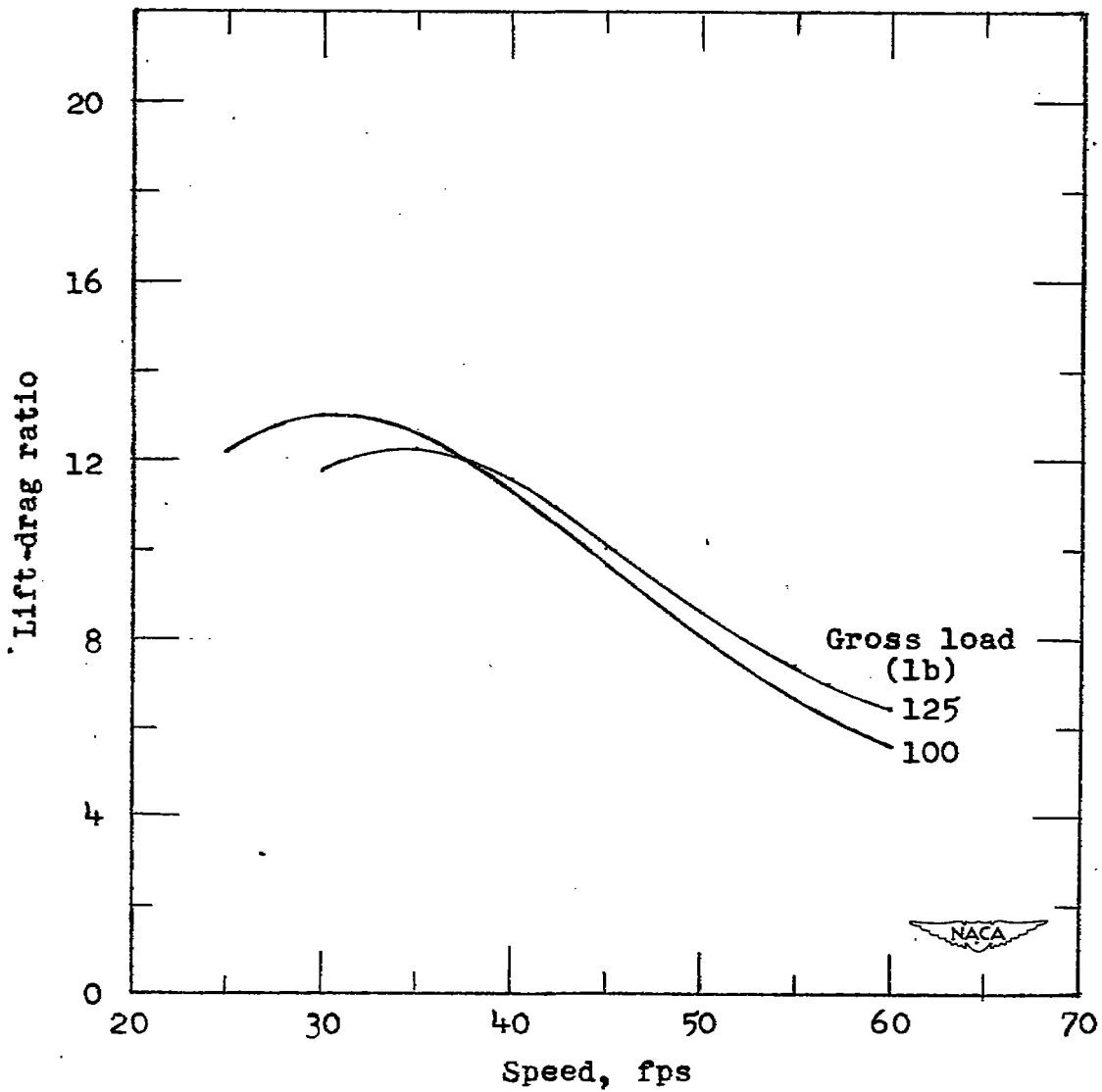
(b) Drag.

Figure 17.- Continued.



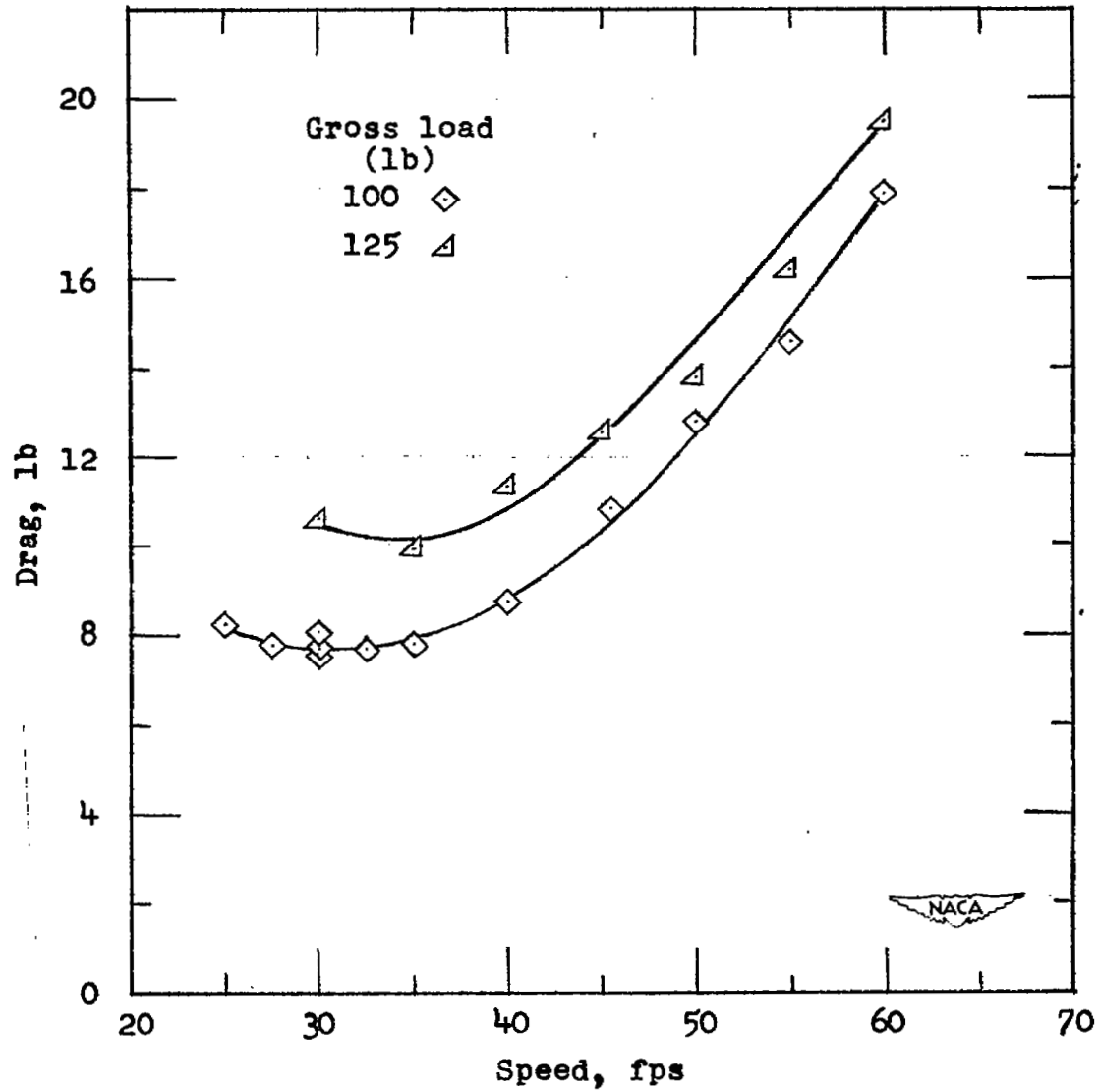
(c) Trim.

Figure 17.- Concluded.



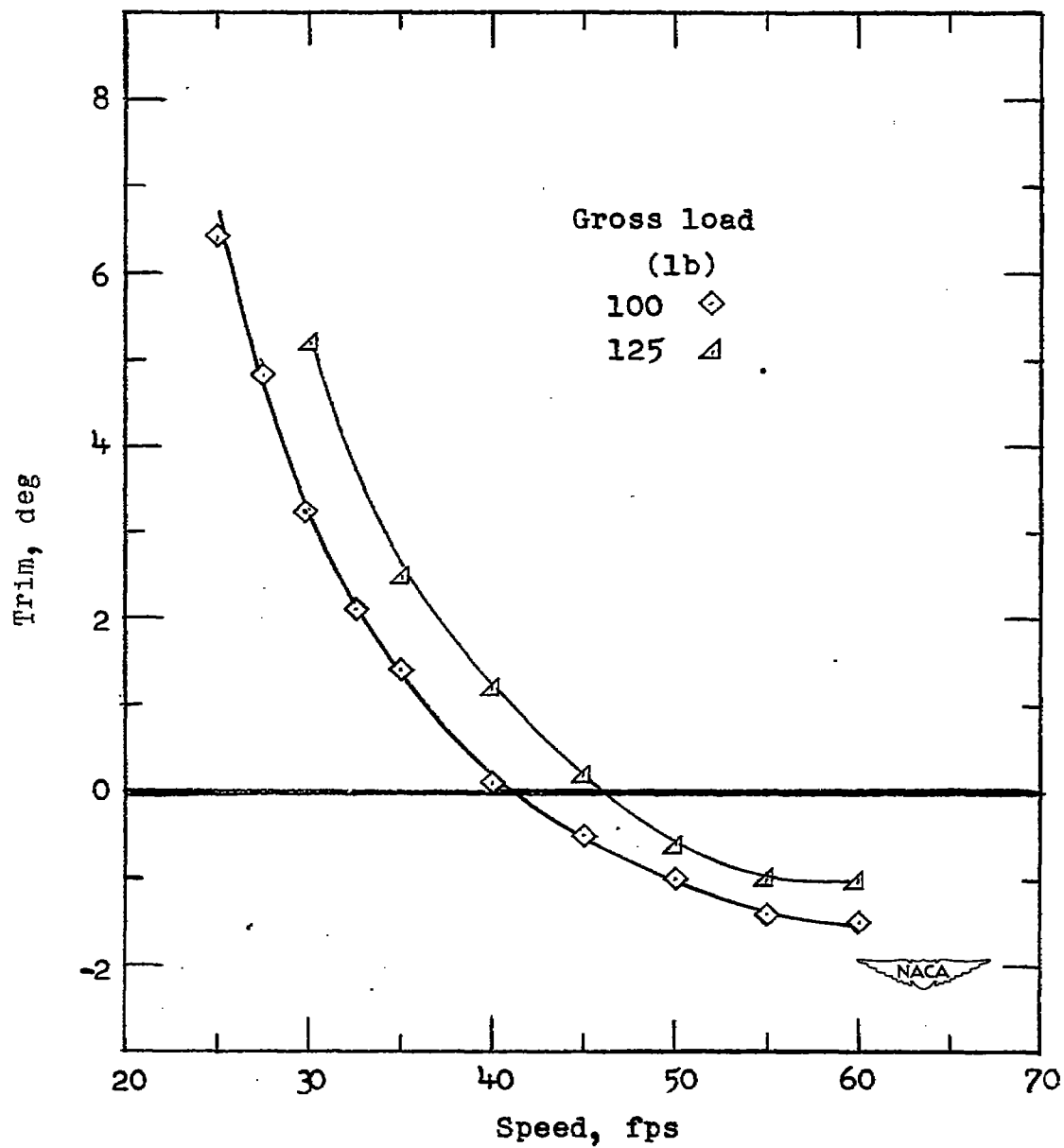
(a) Lift-drag ratio.

Figure 18.- Effect of increase in gross load from 100 to 125 pounds.
Stabilizer A; $l_{cg} = 90$.



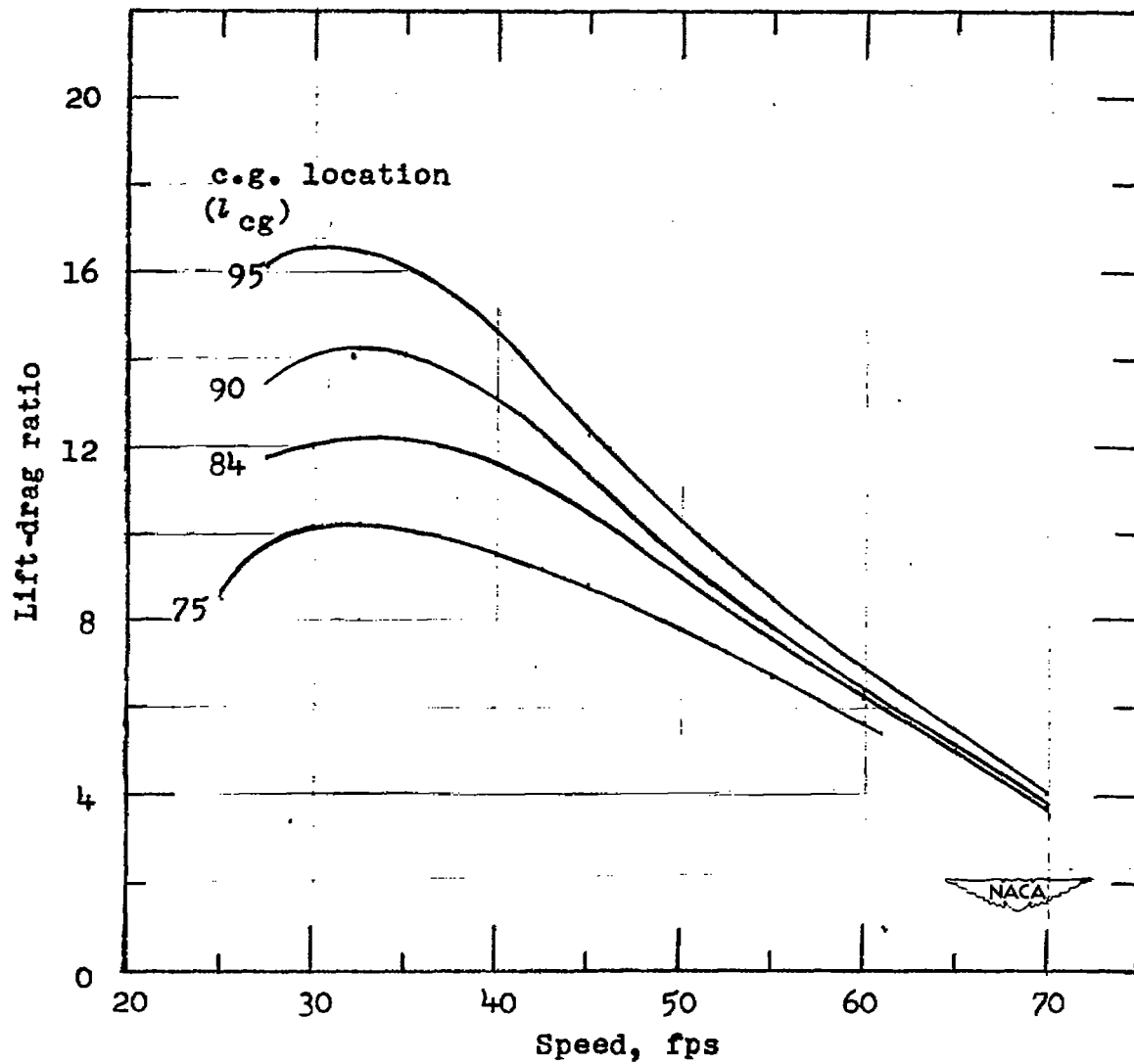
(b) Drag.

Figure 18.- Continued.



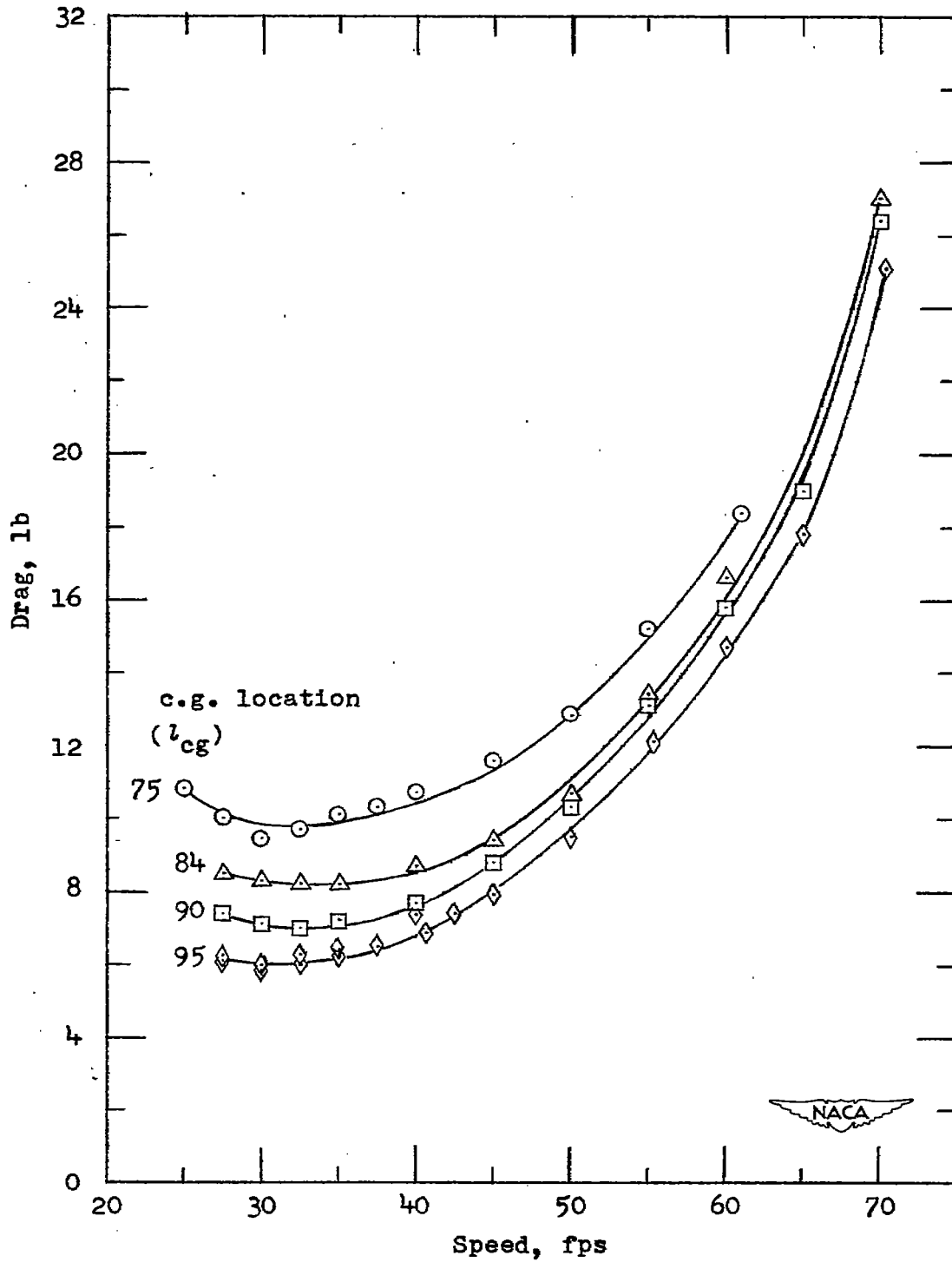
(c) Trim.

Figure 18.- Concluded.



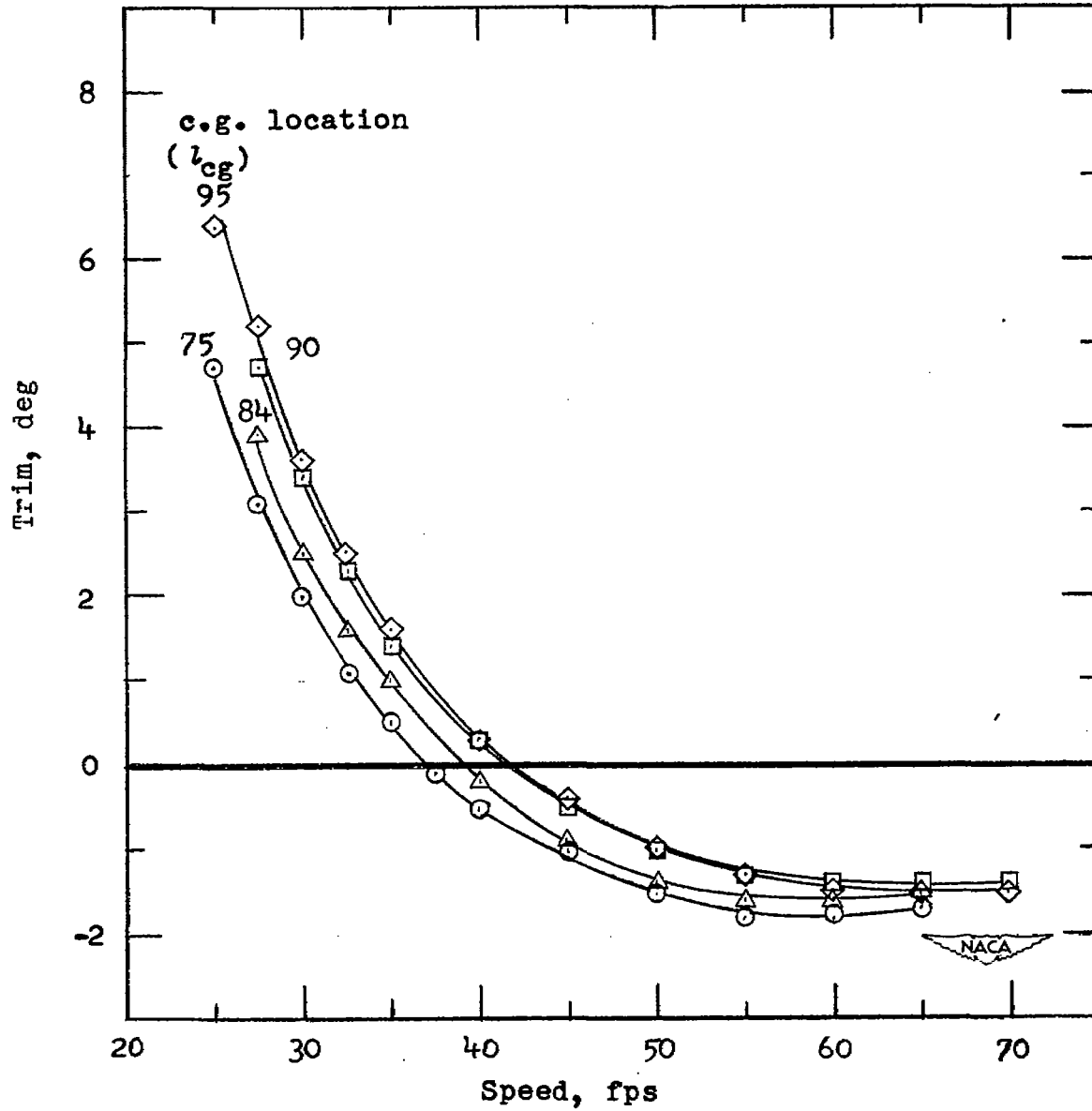
(a) Lift-drag ratio.

Figure 19.- Effect of center-of-gravity location. Stabilizer B.



(b) Drag.

Figure 19.- Continued.



(c) Trim.

Figure 19.- Concluded.

SECURITY INFORMATION

NASA Technical Library



3 1176 01436 4625

